IN VITRO EXPLORATION OF FUNCTIONAL ACROLEIN TOXICITY WITH CORTICAL NEURONAL NETWORKS

Stormy Durant

Thesis Prepared for the Degree of

MASTER OF SCIENCE

UNIVERSITY OF NORTH TEXAS

May 2018

APPROVED:

Guenter W. Gross, Major Professor
Amie Lund, Committee Member
Ernest J. Moore, Committee Member
Art Goven, Chair of the Department of Biological Sciences
Su Gao, Dean of the College of Science
Victor Prybutok, Dean of the Toulouse Graduate School

Durant, Stormy. *In Vitro Exploration of Functional Acrolein Toxicity with Cortical Neuronal Networks*. Master of Science (Biology), May 2018, 55 pp., 8 tables, 26 figures, references, 58 titles.

Acrolein is produced endogenously after traumatic brain injury (TBI) and is considered a primary mechanism for secondary damage occurring after TBI. We are using frontal cortex networks derived from mouse embryos and grown on microelectrode arrays in vitro to monitor the spontaneous activity of networks and the changes that occur after acrolein application. Networks exposed to acrolein exhibit a biphasic response profile. An initial increase in network activity, followed by a decrease to 100% activity loss in applications ≥ 50 µM. In applications below 50 µM, acrolein was not toxic but generated activity instability with coordinated but irregular population busts lasting for up to 6 days. The increase in activity preceding toxicity may be linked to a decrease in free spermine, a free radical scavenger that modulates Na+, K+, Ca+ channels as well as NMDA, Kainate, and AMPA receptors. Action potential wave shape analysis after 20 and 30 µM acrolein application revealed a concentration-dependent 15-33% increase in peak to peak amplitude within minutes after exposure. For the same concentrations of acrolein (50 µM), the time required to reach 100% activity loss (IT_{100}) was longer in serum-free medium than in medium with 5% serum, in which IT_{100} values were reduced by a factor of 4. The greater toxicity in the presence of serum may be explained by acrolein adducts on serum proteins. These reaction products have been shown by other labs to be toxic in cell culture. This in vitro system could be used to expand biochemical analyses such as acrolein-induced spermine depletion and may

provide an effective platform for investigating cell culture correlates of secondary TBI damage.

TABLE OF CONTENTS

Page

LIST OF TABLES

Page

LIST OF FIGURES

Page

CHAPTER 1

INTRODUCTION

Reactive aldehydes are a biomarker of oxidative stress, generated through several metabolic pathways (Cerevelli, 2004; Murray-Stuart, 2004; Wood, 2007). Acrolein is the most reactive aldehyde, and is a more potent toxicant than hydrogen peroxide in cell culture (Sharmine et al 2001). It catalyzes reactive oxygen species (ROS), possesses a half-life that is orders of magnitude greater than any known ROS, can continue self-propagation through initiation of lipid peroxidation and ROS formation, and is further generated by oxidase enzyme up-regulation (Ghilarducci et al., 1995). The presence of acrolein within a cell is followed by an ionic imbalance, ATP depletion, proteolysis and oxidative stress (Sullivan et al., 1998). Exogenous exposure to aldehydes or acrolein can induce oxidative stress and acrolein generation within tissues of all types (LoPachin & Gavin, 2014).

In chemical structure, acrolein is the smallest aldehyde and is a strong electrophile, meaning it is electron deficient. This property makes acrolein seek an (electron rich) nucleophile to covalently bond via Michaels addition (Lopachin & Gavin, 2014). Adducts of acrolein inactivate and impair enzymes, DNA, and structural proteins inhibiting cellular processes. Mitochondria, thiol groups and cysteine amino acid residues are normal targets for acrolein adduction. Enzymes and co-factors are inhibited by acrolein adduction, leading to a mitochondrial permeability state and inhibition of ATP production. (Picklo, 2000; Lijuan, 2006; Tsutsu, 2014).

Defense mechanisms exist for electrophilic compounds within the cell. Glutathione transferase is a group II CYP enzyme responsible for deactivation of

electrophilic chemicals. Glutathione is a strong nucleophile that readily conjugates with acrolein and undergoes N-acetylation to produce *S*-(3-oxopropyl)-*N*-acetylcysteine (OPMA). Oxidation of this product to OPMA-*S*-oxide creates an even more toxic compound than acrolein (Stevens & Maier, 2008).

1.1 Significance in Neurophysiology

Acrolein is produced endogenously within neural tissue after traumatic brain injury (TBI) and is a biomarker for head or spinal injury (Tsutsui, 2014; Shi et al., 2015; Cebak et al., 2016). Acrolein and its aldehyde derivatives were found to be the primary mechanism for secondary damage that occurs weeks to months after a TBI, concussion, or surgical procedure on the spine (Cebak et al., 2016). This chemical is also found in high concentrations in neurodegenerative diseases (i.e. Alzheimer's, Parkinson's, multiple sclerosis, stroke and vascular ischemia).

There is an abundance of literature on the cytotoxic mechanisms of acrolein. Very little literature on the functional effects of acrolein on electrically excitable cells, such as neurons, exists within current literature. Now I will cover the known mechanisms by which acrolein can induce excitotoxicity, increasing secondary damage after the initial physical insult.

There is a period of increased NMDA receptor activation and associated excitotoxicity after TBI, this lasts for only a few hours in a mouse model, and 1-2 days in a human model. This is followed by electrophysiological inhibition (Bullock et al., 1992; Biegon et al., 2004; Krishnamurthy et al., 2016). The same functional manifestations have been implicated in stroke and cerebral ischemia, where acrolein is also produced

endogenously. There is no current knowledge on the functional response of networks when exposed to acrolein in neural tissue. This response is life threatening and, in a laboratory setting, has value for developing innovative pharmacotherapy to treat secondary damage after sustaining a TBI.

Acrolein is generated by and catalyzes lipid peroxidation, also forming free radical reactions. Following a TBI, increased activity of amine oxidase (AO) and spermine oxidase (SO) produces excess acrolein as a byproduct of enzymatic catalysis (Tomitori, 2005; Caldwell, 2015). These enzymes are important in the production of polyamines. Polyamines are found in all human tissue systems, with the highest concentrations found in brain tissue. They play a regulatory role in the membrane potential and action potential production of neurons.

Spermine, a polyamine, modulates the N-methyl-D-aspartic acid (NMDA) receptor function as well as inwardly rectifying potassium channels (Zapia et al., 1980; Morris & Mayer, 1993; Tsutsui, 2014). Spermine also plays a regulatory role in sodium (Na^+) channels; and its depletion has shown to increase spontaneous spiking and hyper-synchronized discharge in cortical neurons (Fleidervish et al., 2008). Spermine is present at a 2.0 mM concentration within the nucleus and is released during oxidative stress because it functions as a *direct free radical scavenger* (Ha et al., 1998). Tsutsui, 2014 demonstrated: acrolein adducts to spermine and other polyamines via Michaels addition. The amine-acrolein adducts polymerize in favor the formation of diazacyclooctanes. The decrease in free spermine within a neuron would lead to an increase in spontaneous spiking and coordinated bursting, increasing NMDA activation, AO and SO activation, ROS formation and ultimately oxidative stress.

The presence of NMDA receptor hyper-activation and excitotoxicity after a TBI in mice has been implicated along with the process of secondary damage (Beigon et al., 2004, Krishnamurthy et al., 2016). Increased activation of NMDA receptors and excitotoxicity have been classified as key components to the pathophysiology of secondary damage after TBI (Yi & Hazell, 2006; Werner & Engelhard, 2007; Greve & Zink, 2009). The latest key component to secondary damage, the presence of acrolein, was published in 2016 (Cebak et al.). Free radical scavengers were able to mitigate the typical degeneration seen post TBI (ibid).

The increase in PO, ROS, and acrolein activates microglial cells which induce genetic changes in surrounding astrocytes (Patel, 2016). These changes create a pathogenic astrocyte, labeled A1, which alters transcription to inhibit the abilities of facilitating neuronal survival, outgrowth, synaptogenesis and phagocytosis (Liddelow, 2017). The astrocytic glutamate transporter is down regulated in A1 astrocytes, leaving excess glutamate in the synapse (Yi & Hazell, 2006; Landgehem, 2006; Lin, 2012; Guerriero, 2015). This means that oxidative stress from increased activity could promote the further generation of acrolein, a self-catalyzing compound with the longest half-life of any ROS.

Post TBI induced epilepsy is positively correlated with TBIs that include hemorrhaging. In the literature, a 24-hour window exists for treatment to avoid post TBI induced epilepsy and this is suggested by the death of important inhibitory interneurons (which are highly sensitive to oxidative stress) during TBI induced excitotoxicity (Sloviter, 2011). Langer et al demonstrated in 2011 that treatment with a low affinity, noncompetitive NMDA antagonist in the first 24 hours after TBI reduced the death of

important inhibitory interneurons. This also reduced post TBI induced epilepsy (Langer et al., 2011).

The project represents an *in vitro,* exogenous exposure to acrolein in murine mouse frontal cortex neuronal networks for quantitative insight into the functional changes that occur in electrophysiology generation of acrolein. The biochemical nature already known about this compound in current literature reveals a possibility that acrolein can induce functional changes important in the process of secondary damage and degeneration following a physical insult. This study aims to elucidate the functional changes when acrolein is added to a neuronal network without any of the other variables which are generated along with TBI.

CHAPTER 2

METHODS

2.1 Microelectrode Array (MEA) Fabrication

All MEAs used in this study were fabricated in the Center for Network Neuroscience (CNNS) photolithography laboratory at the University of North Texas by undergraduate volunteers (Christopher Pino and Jake Gray). The MEA fabrication technique has been published in detail previously (Gross, 1979; Gross et al 1985; Gross, 1994).

MEAs are 5 x 5 cm glass plates coated with of film of indium-tin oxide (ITO). Conductors are photoetched and then insulated with 2-3 mM thick polysiloxane resin (methyltrimethoxysilane). The electrodes are constructed by laser de-insulation which creates 20 mM diameter craters. The exposed ITO is coated with gold to decreased impedance. The center of the MEA has a 1.0 mm^2 recording area comprised of 64 microelectrode terminals.

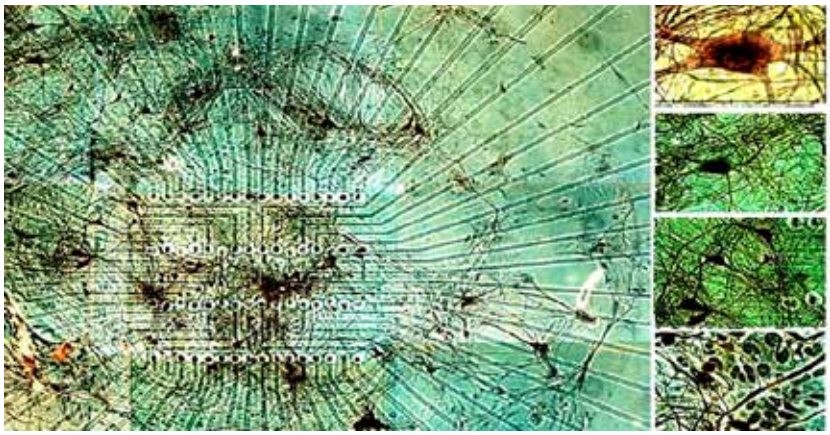

Fig. 2.1. Neuronal cells on a 64 electrode micro electrode array (MEA). Bodian stain. CNNS archives.

2.2 Frontal Cortex Cell Culture

The frontal cortices of E16 mouse embryos are isolated in a sterile balanced salt solution, dextrose-1, sucrose, glucose, and HEPES buffer (D1SGH). This solution moistens and stabilizes the osmolarity of the tissue for mincing with surgical scalpels. The D1SGH is aspirated and replaced with 5.0 ml of 0.05% trypsin and 1.5% DNase II solution. The minced tissue is incubated for 13 minutes at 37 ^{o} C. The entire solution is aspirated by pipette and replaced by 5.0 ml of Dulbecco's modified Eagle medium (DMEM). Tissue is given 3.0-5.0 minute to settle at the bottom of the 15 ml centrifuge the medium is then aspirated and replaced by fresh DMEM. This new suspension is given 3.0-5.0 minutes to settle and then the medium is aspirated and replaced by 8.0 ml of DMEM. The tissue is triturated gently, 5.0-7.0 times, then sampled for cell count on the hemocytometer. Cell density is adjusted to 70,000 cell per 100 (700,000 cells per ml) using DMEM for dilution of cells. Cells are pipetted onto MEAs (previously coated in poly-D-Lysine and laminin), in a 100 µL volume and incubated at 38.0 ^{o} C in 10% CO_2. After 1.0-2.0 hr for adhesion, cells receive a 3.0 ml volume of DMEM with 5.0-10% fetal bovine serum. Cells develop in this medium until the third day *in vitro* (DIV). At this point, the medium is exchanged with DMEM with 5% horse serum. Routine feeding is conducted biweekly.

Once the glial carpet is 100% confluent, serum is decreased to 2% for control of glial cell growth. Networks are allowed 4 weeks to develop before experimentation. $GABA_a$ agonists and antagonists are used routinely to test pharmacological responses of cultured networks.

2.3 Selection of a Network for Experimentation

Phase contrast microscopy is used to monitor network growth and development. When the network has fully developed (~ 4 weeks), selection is based upon a criterion that combines microscopy and laboratory equipment. This is necessary for time efficiency as well as experimental success. The criteria are based on several parameters.

The first criterion is morphology. Cytoplasmic membrane characteristics, cell density, density of processes connecting cells within the network, stressed or dying cells, activated glial cells and glial carpet density.

The second criterion is the network location. If the network adheres to a location off center from the MEA, no electrophysiological data can be obtained. This makes the culture a candidate for time lapsed microscopy experiments only.

The third criterion is the MEA condition. loss of gold increases the electrode impedance. Cracks lower the shunt impedance, resulting in a loss of signal.,

The fourth criterion is osmolarity. Sampling of 10 µL network medium inside the clean room is taken outside to be measured by the osmometer.

If a culture passes all four of these criteria, it is selected for experimental setup. Further selection methods are discussed in the next section, once electrophysiological data is available.

2.4 Electrophysiological Monitoring

MEAs with mature, monolayer networks have pharmacological histiotypic electrophysiological responses, like the parent tissue (Gross et al.,, 1993; Gross &

Gopal., 2006; Potter & DeMarse, 2001; Johnstone et al., 2010). Tissue is transferred from a Petri dish inside the incubator, into a chamber that functions as an external incubator while allowing for amplification of electronic signals. The chamber is opaque with a window for phase contrast microscopy, closed to external air with an ITO cap to minimize heat loss, dehydration, contamination and maintain constant life support conditions (osmolarity, pH and temperature). The ITO window is heated to prevent condensation and allow microscopic observation during the entire experiment.

The chamber is placed on an inverted, phase contrast microscope to allow for simultaneously electrophysiological and morphological monitoring. Details on the experimental setup have been described previously (Gross and Schwalm, 1994; Gross et al., 1994). Cultures are kept at 37 ^{o} C with a within a range one of $\pm$ 1.0 ^{o} C. A continuous 10 ml/min stream of medical grade 10% CO_2 in air flows into the chamber cap to maintain pH in the range of 7.3 to 7.5. The phenol red indicator of the stock media for pharmacology is used for qualitative measurement of pH for the duration of the experiment. Quantitative hydrogen ion concentrations from pH meters are used to accurately measure medium when a 100 µL volume is available for measurement.

Osmolarity measurements require only a10 µL test volume and could be made through the course of the entire experiment. When measuring osmolarity, to control for sampling errors due to stratification, 50% of the medium is withdrawn temporarily from the chamber and a 10.0 µL volume is taken from this sample.

Two chambers were used for these studies: a single network M-4 chamber with two Luer ports and a total volume of 2 mL, and a dual network M-5 chamber with separate wells of 1 mL volume and two Luer ports each. In each case one port is used

for water addition from a syringe pump to compensate for evaporation and maintain osmolarities. The other Luer port is used for medium changes, extraction of medium samples and test substance application (Fig. 2.1).

Test substance application: 100-300 µL medium sample is withdrawn from the network chamber via the Luer port into a syringe. The syringe is withdrawn and the test substance is injected into the syringe tip ~~by~~ with a micropipette. The syringe with medium is inserted into the chamber Luer port where another small amount of medium is carefully withdrawn and mixed with the medium containing the test substance. The test substance and medium mixture is slowly returned ~~in~~to the network chamber.

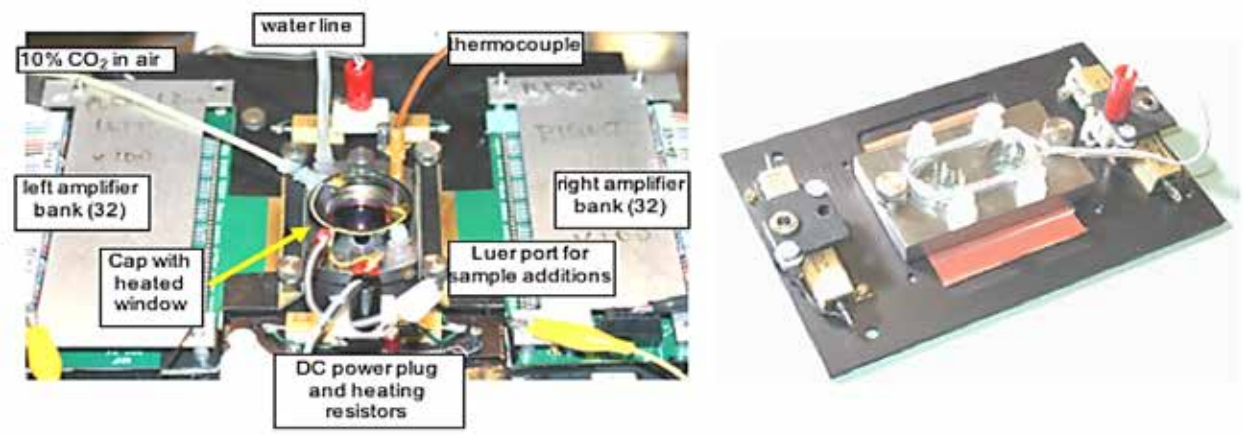

Fig. 2.2. Electrophysiological and life support setup: (Left) M4 chamber which records from a single network. 32 preamplifiers (Plexon Inc.) are attached to either side. (Right) M5 chamber which allows for the recording of two separate networks, each in their own chemical environment. CNNS Archives.

The amplification is achieved in two stages. A 100-fold fixed amplification with 32 preamplifiers positioned to the left and right of the chamber and a variable second stage amplifier that can adjust total amplification up to 20,000. Normal amplification levels are 10,000 to 12,000. Spikes can be identified by wave shapes (wave shape template algorithm, Plexon inc Dallas). With good signal to noise ratios is possible to separate four wave shapes on one physical channel in real time (Fig. 2.3). Primary network

activity is displayed as real time spike raster display from wave shape crossings of a threshold with a resolution of 25 µsec.

An additional custom CNNS program (Vernac) plots total activity or average activity per min which allows visualization of changes in network activity. This is a convenient, simple display used for all experiments.

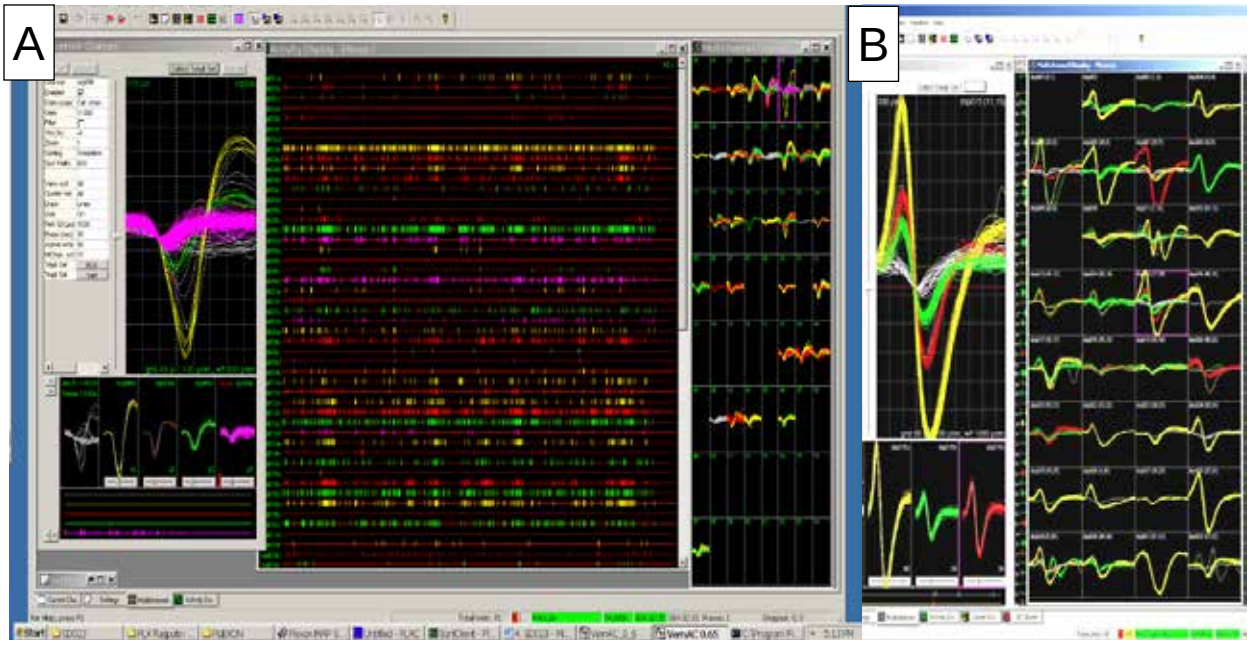

Fig. 2.3. Common displays of the Plexon Omniplex system. (A) Real time extracellular firing of each individual unit that has been selected. (64 channels). (B): High signal to noise ratios (SNR) in a 32-channel recording system. Under these conditions, waveshape separation is possible with high precision and a maximum of 4.

2.5 Methods for Analysis of Electrophysiological Data

Network spike production was plotted as mean or total spikes per minute for the entire experiment. Each minute, the total activity was divided by the active channels (floating average). An active channel was defined as one with at least 10 discriminated spike signals per minute. Such a display allowed the monitoring of the evolution of

activity and represented the primary real time contact with the network. Burst activity was monitored with the Plexon raster display and quantified offline.

Activity from different networks was never pooled, and changes were normalized as percent decreases from network-specific reference activity that was maintained in a stable state for a minimum of 60 min (native activity) before acrolein experiments. Neurophysiological parameters were quantified from spike rate plots using NEX analysis programs (NEX Technologies). All Plexon time stamps are stored with a 25 µs resolution and a raster plot of all channels can be re-created for the entire experiment. Segments of such data are used in several figures in this thesis to depict complex changes in activity. Sigmoidal fits to dose-response data were obtained either with Excel XL Stat and with Origin V-7.

Irreversible activity decreases were obtained at single concentrations and key values were expressed as IT_{100}, i.e. the time when activity had decayed 100%.

2.6 Acrolein Storage, Preparation, and Administration

Table 2.1. Globally Harmonized System (GHS) Hazard Classification of Acrolein

Flammable liquids	Category 2
Acute Oral Toxicity Acute Inhalation Toxicity	Category 2 Category 1
Acute Dermal Toxicity	Category 2
Skin Corrosion	Category 1B
Serious Eye Damage	Category 1
Acute Aquatic Toxicity	Category 1
Chronic Aquatic Toxicity	Category 1

According to the University of California Berkley, it is standard operating procedure to wear gloves, a lab coat, ANSI-approved safety goggles, cotton based clothing and closed toe shoes. Work should take place under a laboratory type fume hood with sash position closed. In order to comply with this, as well as ensure additional protection between fume hood and experiment, a carbon activated mask was an addition to this experiment's standard operations. The CAL/OSHA permissible exposure limit (PEL) is 0.1 ppm (0.25mg/m^3).

Acrolein storage: acrolein is an auto-ignitable auto-oxidant. It must be stored in a cool, dry, hypoxic environment to ensure its stability. Source acrolein bottle must be filled with nitrogen before being placed back into 4-8 ^{o} C.

Table 2.2. Chemical and Toxic Properties of Acrolein

Chemical formula	C_3H_4O
Molecular weight	56.06 g/mol
Melting point/freezing point	-87 ^{o} C (- 125 ^{o} F)
Boiling point	52.2 ^{o} C (125.5 ^{o} F)
Odor threshold	0.21 ppm
Skin protection	Handle with gloves, minimum thickness 0.3 mm
Body protection	A lab coat and sterile sleeves
Respiratory protection	Carbon activated gas mask
USA. Occupational Exposure Limits (OSHA) - Limits for Air Contaminants ACGIH Threshold Limit Values (TLV)	0.10 ppm 0.250000 mg/m3 0.10 ppm

Each experiment required a new solution because of the instability and high reactivity of acrolein. Depending on the experimental concentration, either ultrapure H_2O or DMEM stock solutions was used to dilute the source acrolein solution. Sterility

procedures are maintained between the source acrolein bottle (Sigma) and solution (DMEM or ultrapure H_2O).

Table 2.3. Acrolein Solution Prep

Chemical	Solvent(s)	40 mM Bicuculline (in Network Prior)
Acrolein Diethyl Acetate (Stabilized in 4% Hydroquinone) (ADA)	DMEM with 5% serum DMEM stock (serum free)	yes
Acrolein (stabilized in 10% Hydroquinone) AHQ	DMEM stock (serum free) Ultrapure H_2O	yes
Analytical Acrolein	Ultrapure H_2O	no

CHAPTER 3

RESULTS

The following results were obtained with a cell culture model that has shown utility for exploring the origins of spontaneous activity and study the internal dynamics of neuronal ensembles. It has also found realistic applications to pharmacology and toxicology. This approach provides the unique ability to simultaneously record electrophysiological data derived from frontal cortex networks while observing the network morphology. This is not possible in any in vivo model system due to the biological complexity. Data is presented in 4 sections representing the 4 different chemicals tested: acrolein diethyl acetate (ADA), acrolein stabilized in hydroquinone (AHQ), analytical (pure) acrolein (AA), and hydroquinone (HQ). The latter substance was investigated to determine if it contributed to the toxicity seen in AHQ and ADA experiments because their use as a stabilizer. Each section will begin with a table of experiments, show electrophysiology responses, dose response curves, and conclude with microscopy.

3.1 Acrolein Diethyl Acetate (ADA)

Acrolein diethyl acetate is a similar, but larger and less volatile aldehyde in comparison to acrolein itself. It is stabilized in 4% HQ to prevent auto-oxidation of the compound. A protocol for a single application of ADA and utilizing the response variable of time was constructed in this process.

Table 3.1. Table of ADA Experiments

Exp.	ADA (mM)	# of Channels	Culture date	Exp. Date	Age (days)
MA005	44	33	1.19.16	3.2.16	41
MB005	88	27	1.19.16	3.2.16	41
MA006	47.6	36	1.19.16	3.10.16	49
MA004	7	37	1.19.16	2.24.16	28
MA011	120	37	2.2.16	3.23.16	49
MB011	240	22	2.2.16	3.23.16	49
MA014	47	33	1.19.16	4.5.16	84
MA008	12	23	2.2.16	3.15.16	42
MA007	34	30	2.2.16	3.16.16	43
MB007	34	5	2.2.16	3.16.16	43
MA009	1	45	2.2.16	3.17.16	44
MB009	1	32	2.2.16	3.17.16	44
MB009B	1,000,000	32	2.2.16	3.17.16	44
MA010	6	12	2.2.16	3.18.16	45
MA012	30	0	2.2.16	3.28.16	55

3.1.1 ADA Response Profiles

Fig. 3.1 shows the reduction in spike activity from four different networks exposed to different concentrations of ADA. Percent loss of activity is plotted against time on a linear scale. In this case, a 50% loss is identified as an IT_{50}. Whereas the activity decrease is concentration dependent, with higher concentrations leading to a more rapid loss of activity, the effect of serum was unexpected and is paradoxical., The two experiments in serum-free medium take much longer to lose their activity. Since serum is known to bind a variety of substances, therewith decreasing the effective concentration of the toxicant, it is generally observed that a serum-free environment offers less protection, leading to a more rapid decay of network activity. This is not observed in these experiments and is presently without explanation. The IT_{50} of ADA in the presence of serum is 48 and 90 min for 88 and 44 mM ADA (Fig. 3.1). The IT_{50} of ADA in serum free medium was 225 and 300 min for 50 and 34 mM. This is a

substantial shift, indicating an increased potency in the presence of biomolecules found in serum.

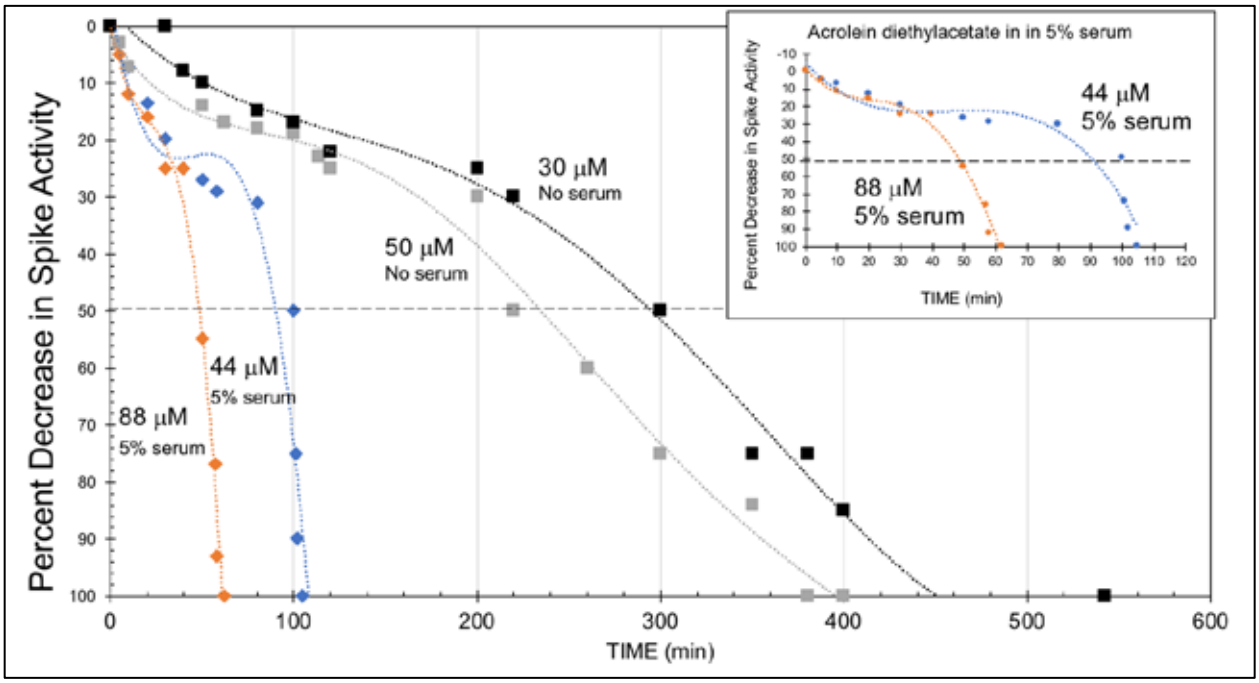

Fig. 3.1. Network activity responses to single ADA applications are concentration and medium dependent. Linear plots with polynomial fitting show expected concentration-dependence but paradoxical effects of serum-containing medium. IT50 values at 44 and 88 mM in serum are 90 and 50 min respectively. In serum-free medium IT50 values at 30 and 50 mM are 300 and 235 min, respectively. The insert amplifies the two response curves obtained in serum-containing medium. NOTE: serum-free responses were biphasic (not shown; ~10-20% increases for 50-100 min).

Fig. 3.2 plots the IT_{100} values for all ADA experiments with single applications (n=6). In the range from 6 mM to 1 Molar, a log-log plot provides a linear function. Two experiments received a full medium change :10 and 6 hr after ADA application. These data points (see triangles) remain on the trend line, indicating that the toxicity of ADA is established at an early time (perhaps less than 15 min) and cannot be reversed by medium changes.

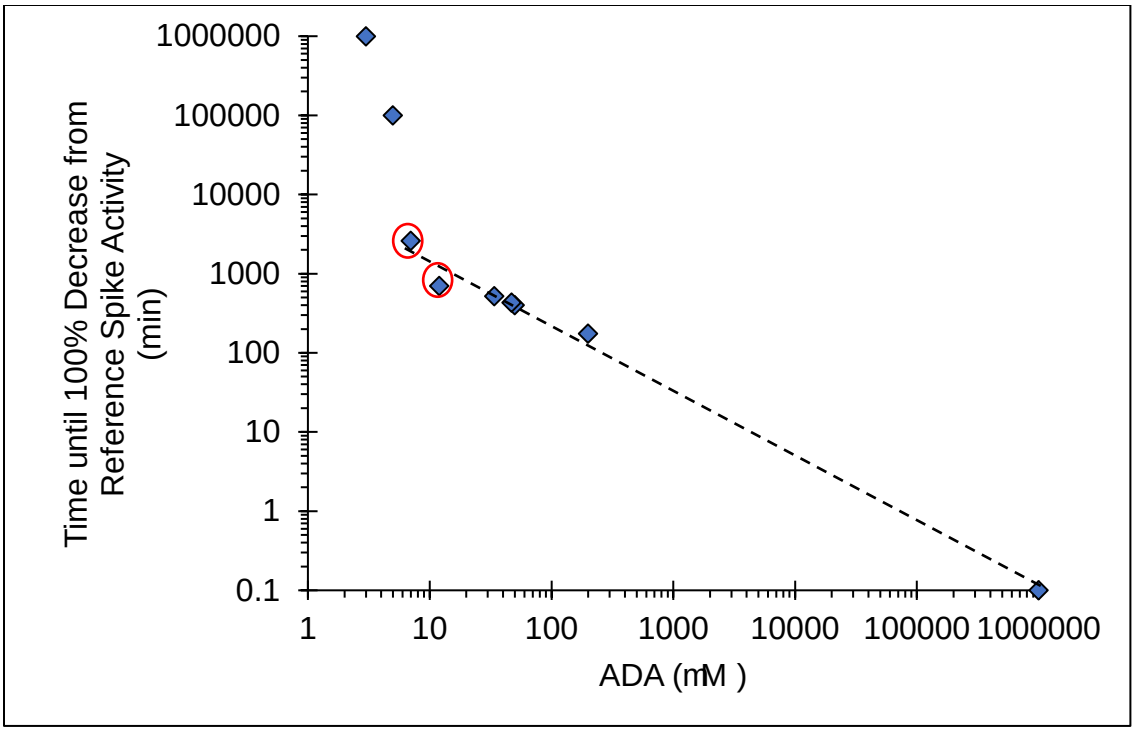

Fig. 3.2. Log-log plot of the time until 100% activity decrease vs ADA concentration in serum-free medium). Two experiments received a medium change: 10 min after 12 mM and 6 hr. after 7 mM ADA application (circled markers above). However, spike termination does not deviate from the log-log function. These observations imply that the ADA effect is established very early after exposure and cannot be reversed by medium changes.

The raw data that has led to the graphs shown in Fig. 3.3 is displayed in Fig. 3.3. for the 50 mM serum-free experiment. This sequence of 30 sec time segments shows the increased activity ignored in Fig. 3.3. Burst rates rise temporarily form 36 bpm in the reference state, to 42 bpm 2 min after application and reach 78 bpm at 100 min. The activity decreases thereafter. The IT_{50} level activity shown in Fig. 3.3 D reveals that the decay in bursting is dominated by an increase in burst period as well as by a shortening of the burst duration.

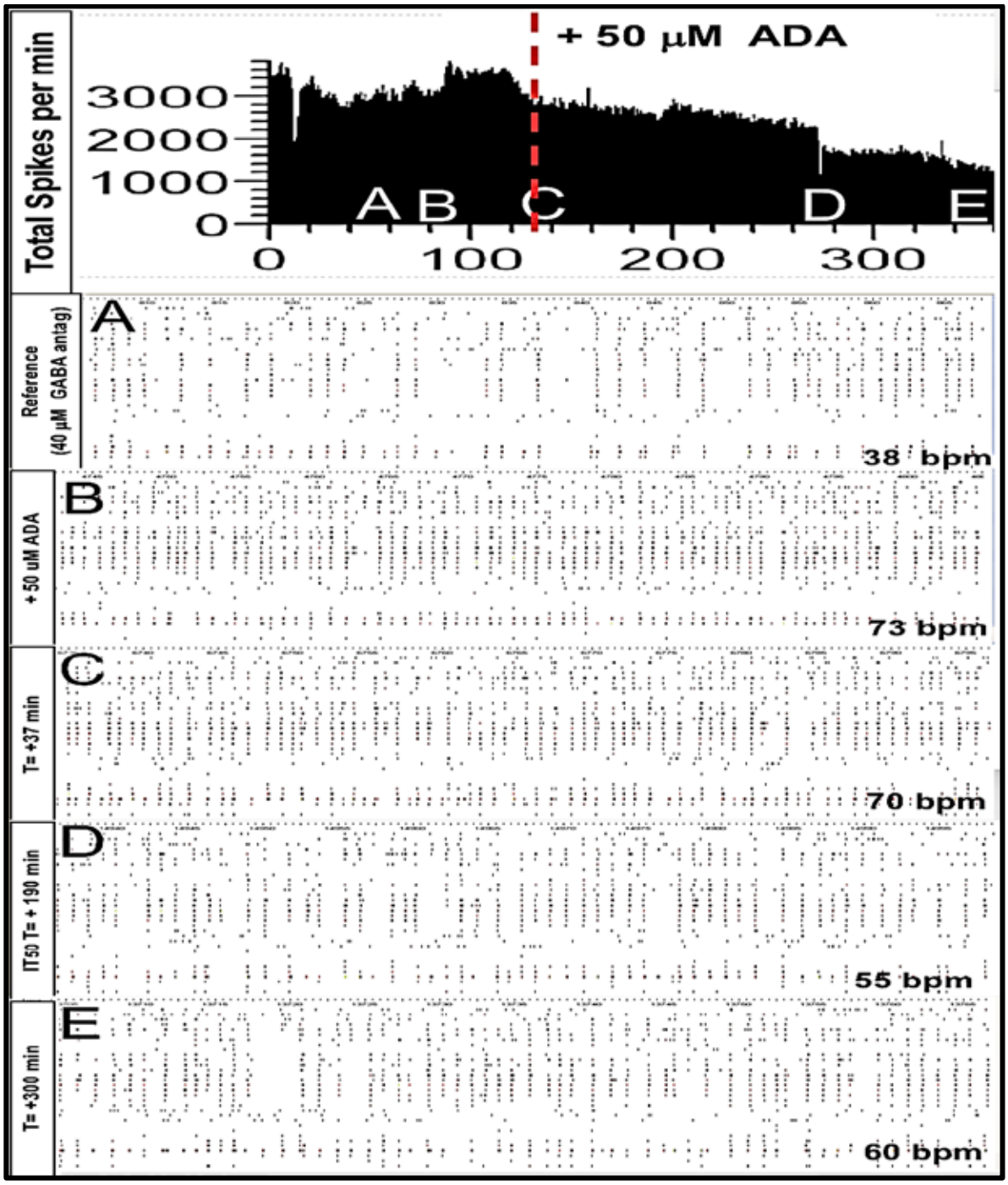

Fig. 3.3. Change in network pattern after 50 mM ADA. Burst rate increases for 50 minutes before decreasing from reference activity range. (A) Raster display of reference spike activity, disinhibited by 40 mM bicuculline. (B) Decrease in period between population bursts 1 minute after 50 mM ADA application. (C) 100 minutes post ADA application showing a continued decrease in spike period without loss of burst coordination. (D) Raster spike display at the IT_{50}. (E) 5 hr after the ADA application.

3.1.2 ADA Dose Responses

Low concentration titrations (3 mM ADA) show no immediate effect in reference spike activity until 24 mM. A decrease in active units is not observed until 45 mM. Two full medium changes could not recover spike activity. The observed EC50 for an instant effect in spike rate from reference after application was 30 mM ADA.

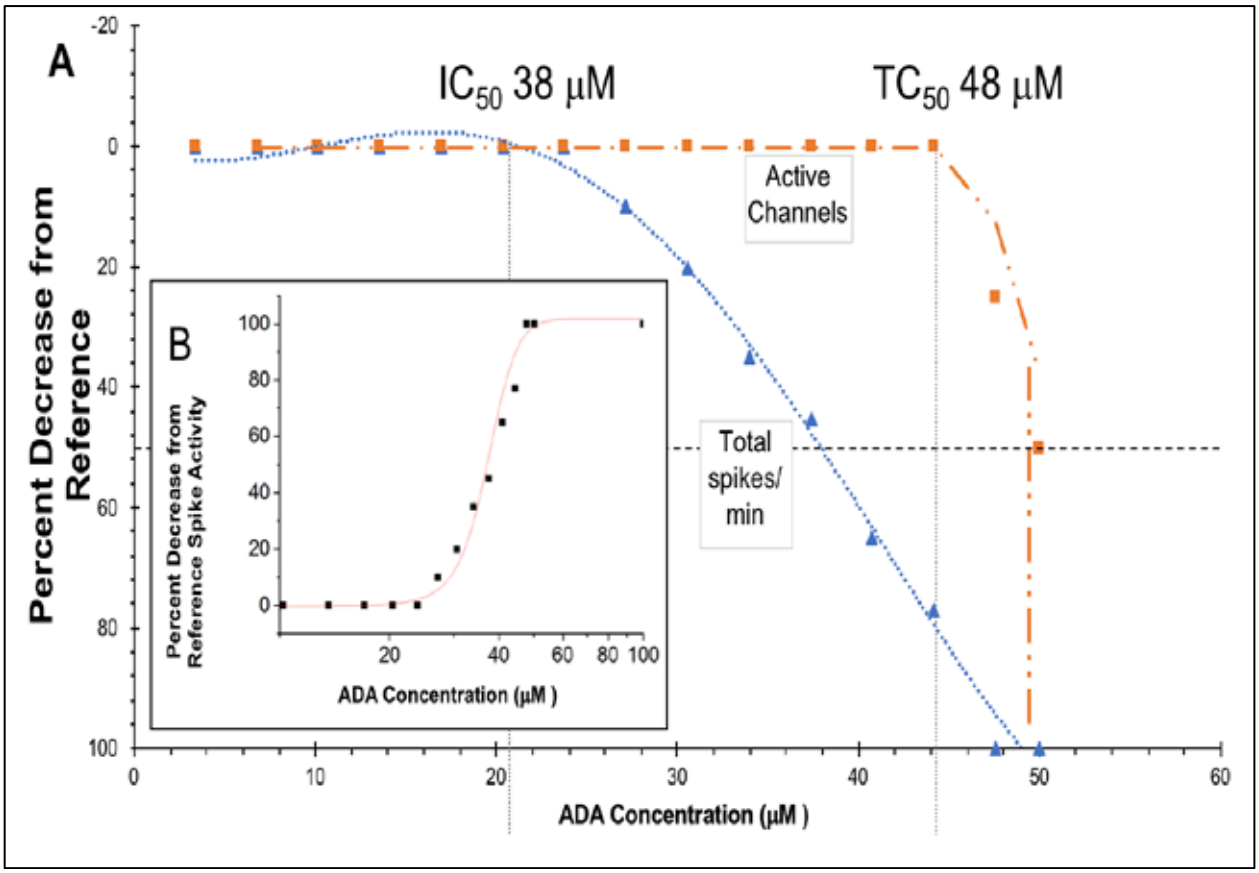

Fig. 3.4. Dose response for ADA on a single culture disinhibited with 40 mM bicuculline. (A) Titrations with 3 mM ADA until the total concentration of 54 mM (18 titrations). Activity loss was irreversible with two medium changes. decrease in spike activity as a function of ADA concentration. The observed IC_{50} was: 38 mM ADA, and TC_{50}: was 48 *mM* (B) Percent decrease from reference spike activity is on the y axis and the concentration increases along the X axis.

3.1.3 Morphological Responses

The time lapse microscopy of ADA experiments exhibited a granular cytoplasm and beading of processes, known as Wallerian degeneration See Fig. 3.5 A and D for the loss of an axon, granulation of the glial carpet, and retraction of the soma from and ovoid shape to a circular one. In the absence of specific staining, axons cannot always be visually identified. However, in all ADA time lapse microscopy, processes extending from cell bodies, would bead and disappear in a time period (n=3).

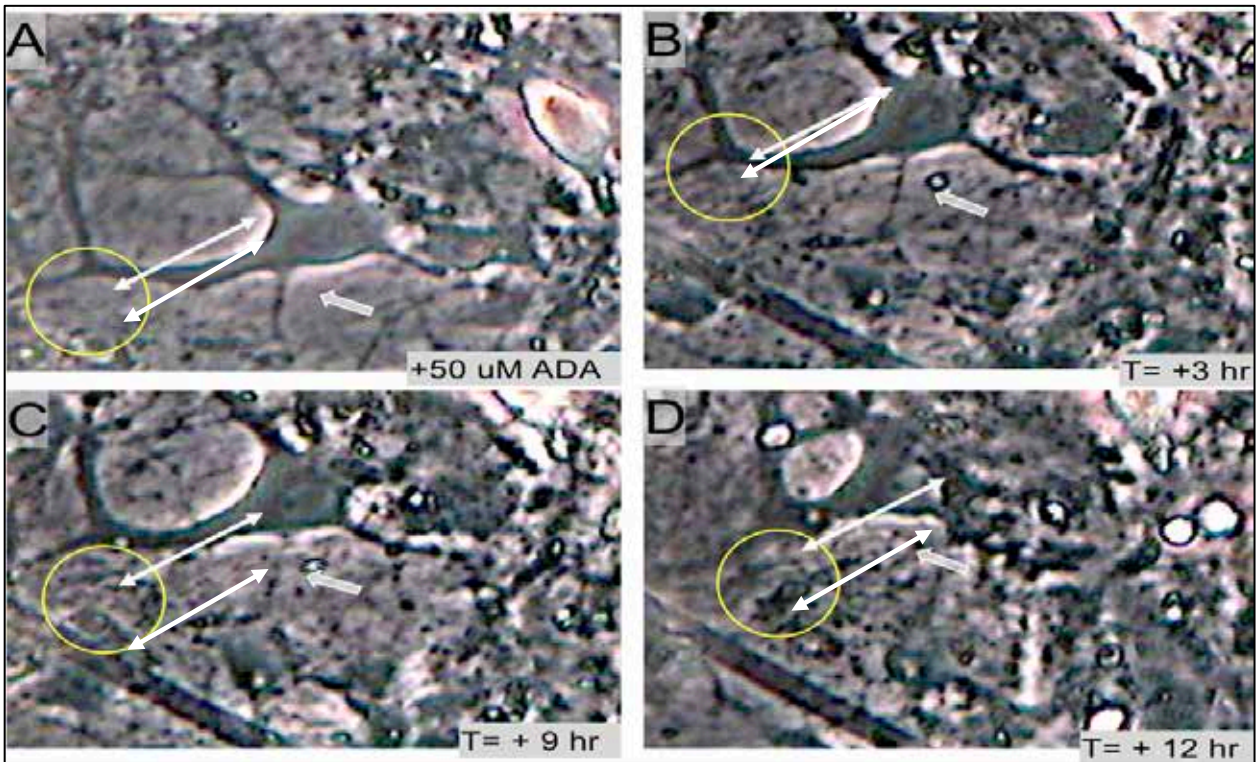

Fig. 3.5. Morphological responses to 50 mM ADA. (A) Directly after dose. White arrow identifies axon. (B) 30 minutes after dose, axon is showing signs of Wallerian degeneration (see insert). (C) Axon has degenerated, leaving debris. (D) Axon debris is gone, full tissue retraction and soma shape changes. The white arrow displayed stays the same length and represents a 50% decrease in space between soma and process.

3.2 Acrolein Stabilized in 10% Hydroquinone (AHQ)

All data on acrolein in 10% HQ is preliminary data. Due to an ongoing backorder, this chemical was unattainable from Sigma Aldrich or Fisher scientific through the period of July 2017-January 2018, when the lab protocol expired and cell culture was permanently closed down. The original July order was cancelled in November 2017 when it was stated by the company that they could not guarantee the shipment of this chemical in the foreseeable future. At this time, the analytical source acrolein became backordered as well.

Table 3.2. Acrolein HQ Experiments

Exp.	Concentration mM	Channels	Culture Date	Experiment Date	Age weeks
MA016	60	30	4.26.16	6.1.16	67
MA017	1,100	21	4.26.26	6.8.16	74
MA018	213	45	4.26.16	6.16.16	82
MA021	2580	17	4.26.16	6.28.16	90
MB021	13200	10	4.26.16	6.28.16	90
MA022	50	22	6.28.16	8.3.16	36
MA019	3,000	Histology	6.28.16	7.27.16	28
MA020	50	Histology	6.28.16	7.28.17	29

3.2.1 AHQ Dose Response

AHQ exhibited a relationship between time and concentration. For concentrations < 2 mM a biphasic profile was observed. First phase: increase in spike activity, followed by a decrease to 100% in spike activity. In concentrations > 2 mM, there rapid loss of activity.

One hundred percent activity loss from reference plotted against AHQ concentration reveals a relationship (in comparable medium), there is a sigmoidal

relationship. The linear segment of the sigmoidal curve has the concentrations 0.5 - 2.0 mM.

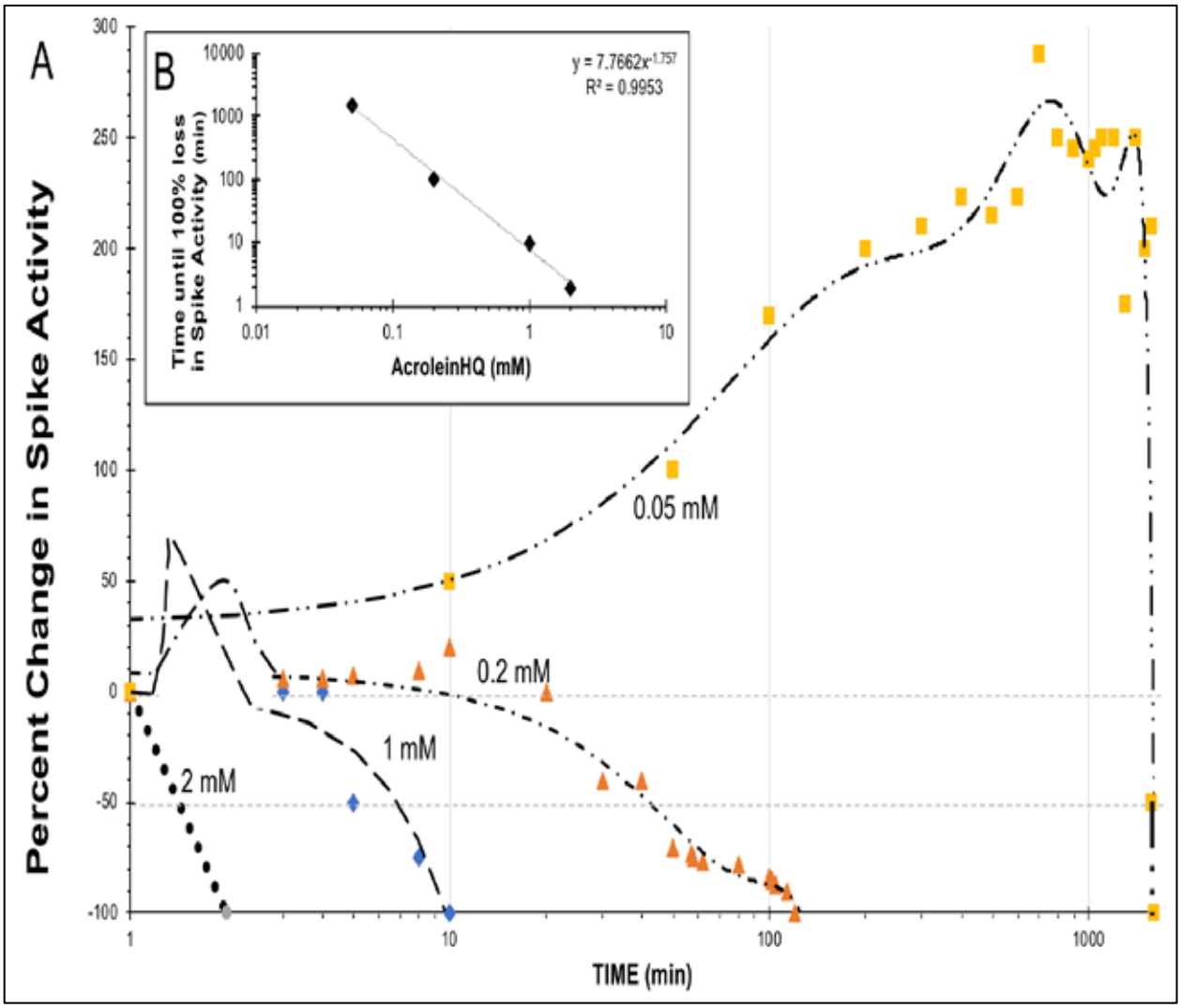

Fig. 3.6. Response in percent change of spike activity from reference after application of AHQ. (A) Lower concentrations exhibit a biphasic response profile. The first profile is an increase in spike rate from reference, followed by a decrease in spike rate and then a decrease in active channels. AHQ concentrations at 2mM cause an instantaneous decrease in spike activity as well as active channels. (B) AHQ concentration is plotted against time until 100% activity loss in experiment that did not contain serum.

After low concentrations of AHQ were applied into network medium, a biphasic response was seen. The first phase began with an increase in spike activity that was followed by a 100% decrease in spike rate.

When 5% serum was added to one experiment, there was no biphasic response profile. The exact same AHQ concentration with serum had a very different profile (Fig. 3.7).

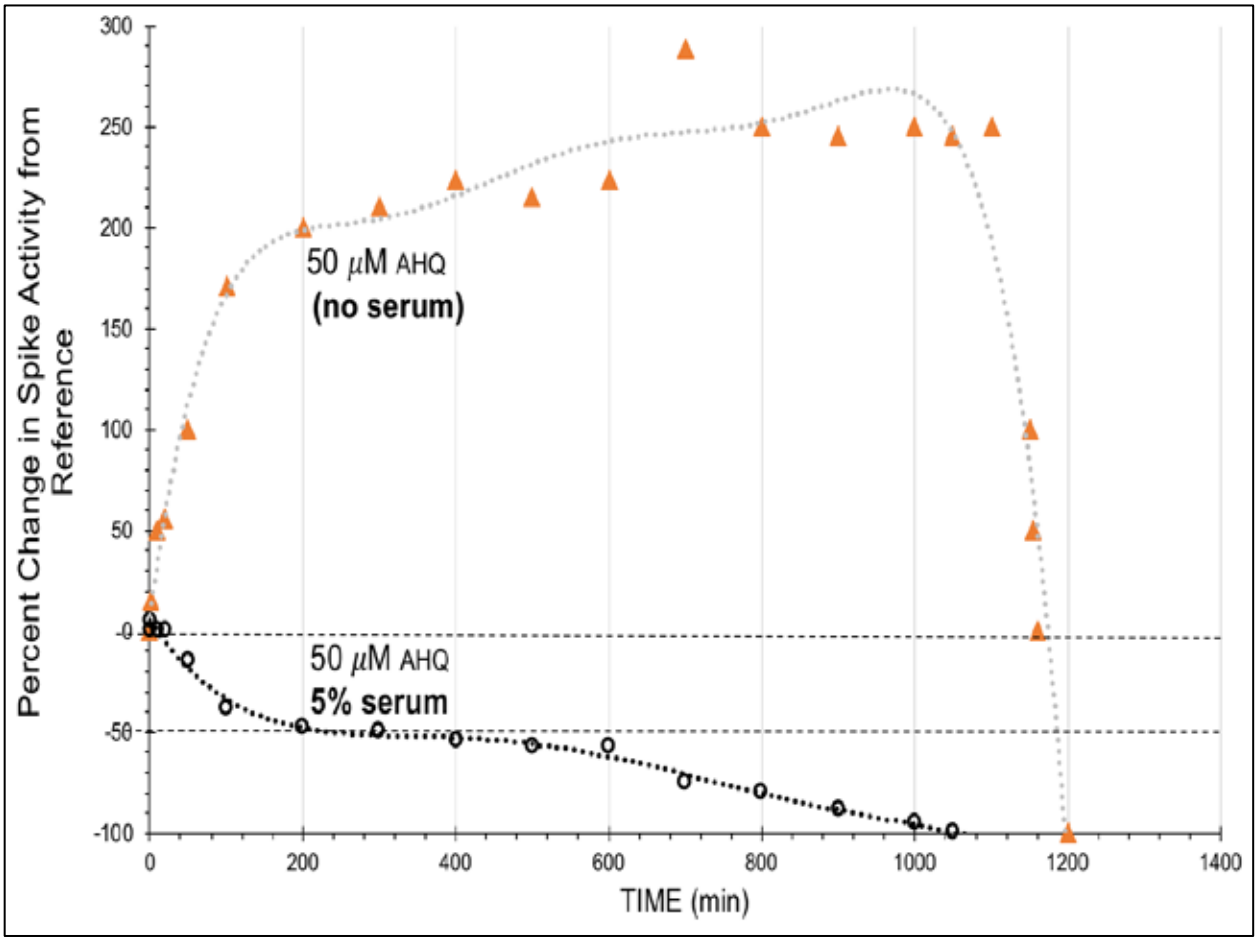

Fig. 3.7. Decrease in spontaneous activity measured as percent of reference overtime for two 50 mM AHQ experiments: one in medium with serum and the other in serum free medium. The IT_{50} with the presence of serum is 350 min, without serum it is 1,200 min

3.2.2 Changes in Network Spike Patterns

Immediately after application, population burst rate increased rapidly and continued to increase during this phase profile. Periods of increased population bursts would dominate the first phase. New units would appear on the oscilloscope that had not been above noise levels prior to application.

At 1.1 mM AHQ, this same profile was observed over a period of 10.0 min. The coordination is sustained until total spike activity is below 90% reference activity. At this point, all activity is lost, and unable to be revived by a medium change. The death profile is either reduction in ignition sites or neural ignition failure.

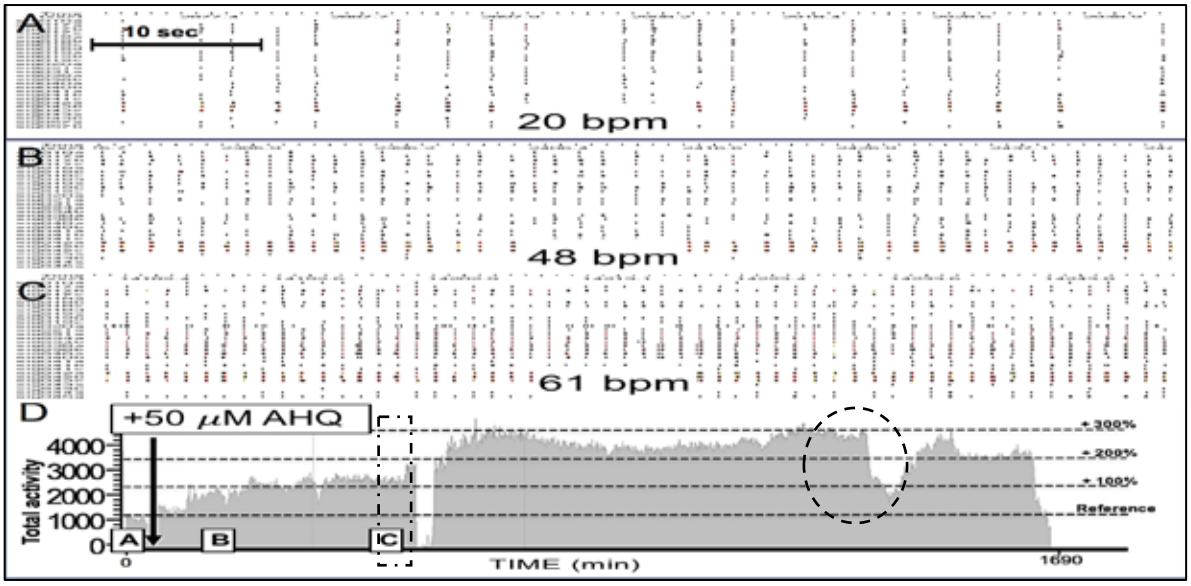

Fig. 3.8. Network spike production and patterns change after 60 mM AHQ. (A) Raster display of spontaneous network spike production, disinhibited by the GABAA antagonist bicuculline (one-minute data segments). (B) After 60 mM AHQ dose, the burst rate increases with time(C) 1,000 minutes after dose: continued inter spike period decrease. (D) The 300% increase of total spike activity over the 1,690 min of activity. The interrupted period of time (rectangle) represents amplifier shutoff for chamber adjustment. The circle shows a temporary decrease from a sudden osmotic shift. A medium change could not reverse the complete lose in spike activity.

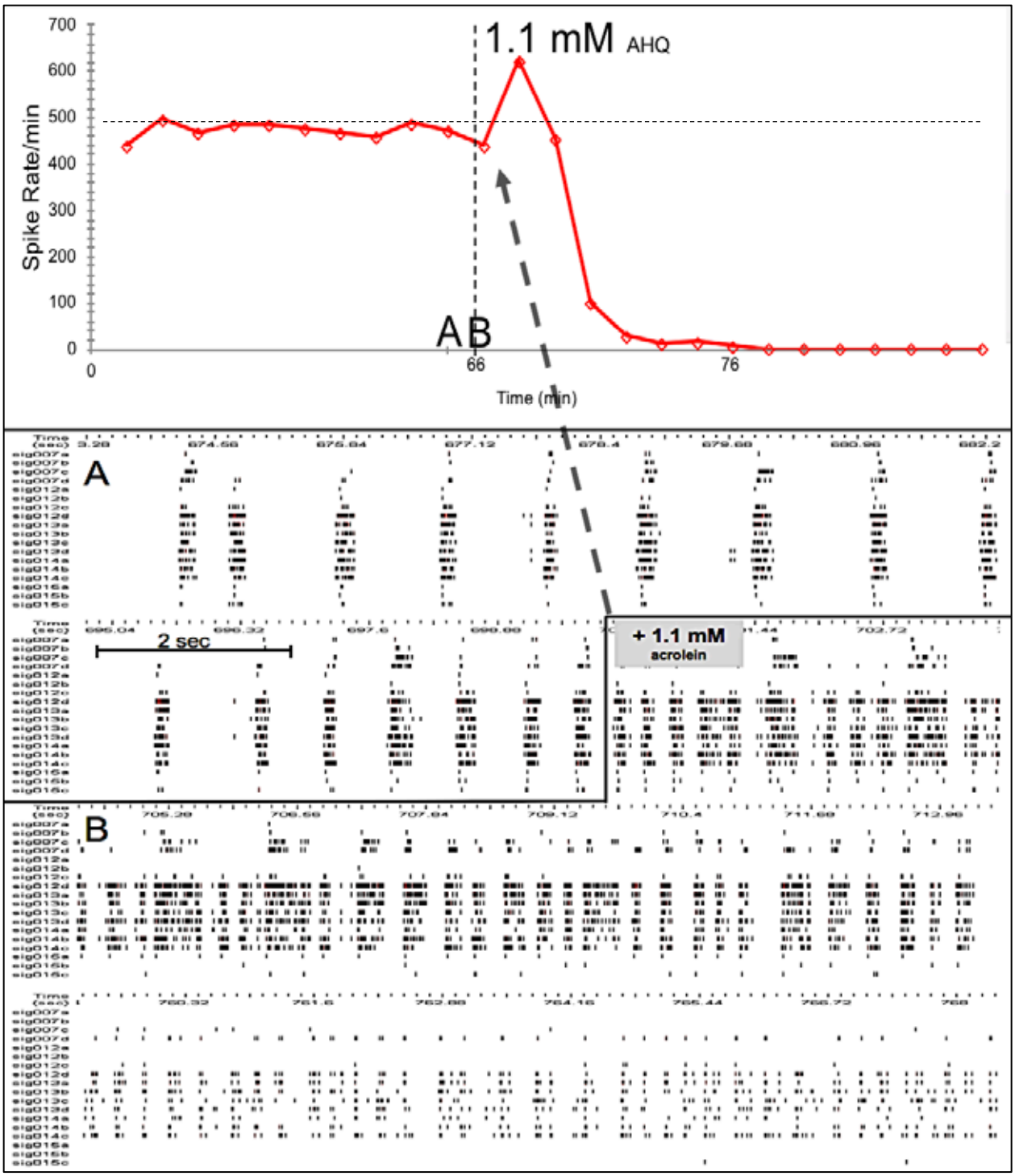

Fig. 3.9. A 1.1 mM AHQ application after 1.0 hr of stable reference spike activity. (A) Raster display of reference burst activity with 40 mM bicuculline. (B) The exact time period of 1.1 mM AHQ application the activity increased from a spike rate of 450 spk/min to 650 spk/min Population burst rate increases rapidly with coordination. Activity decay is characterized decreased burst rate with sustained coordination.

3.2.3 Morphology

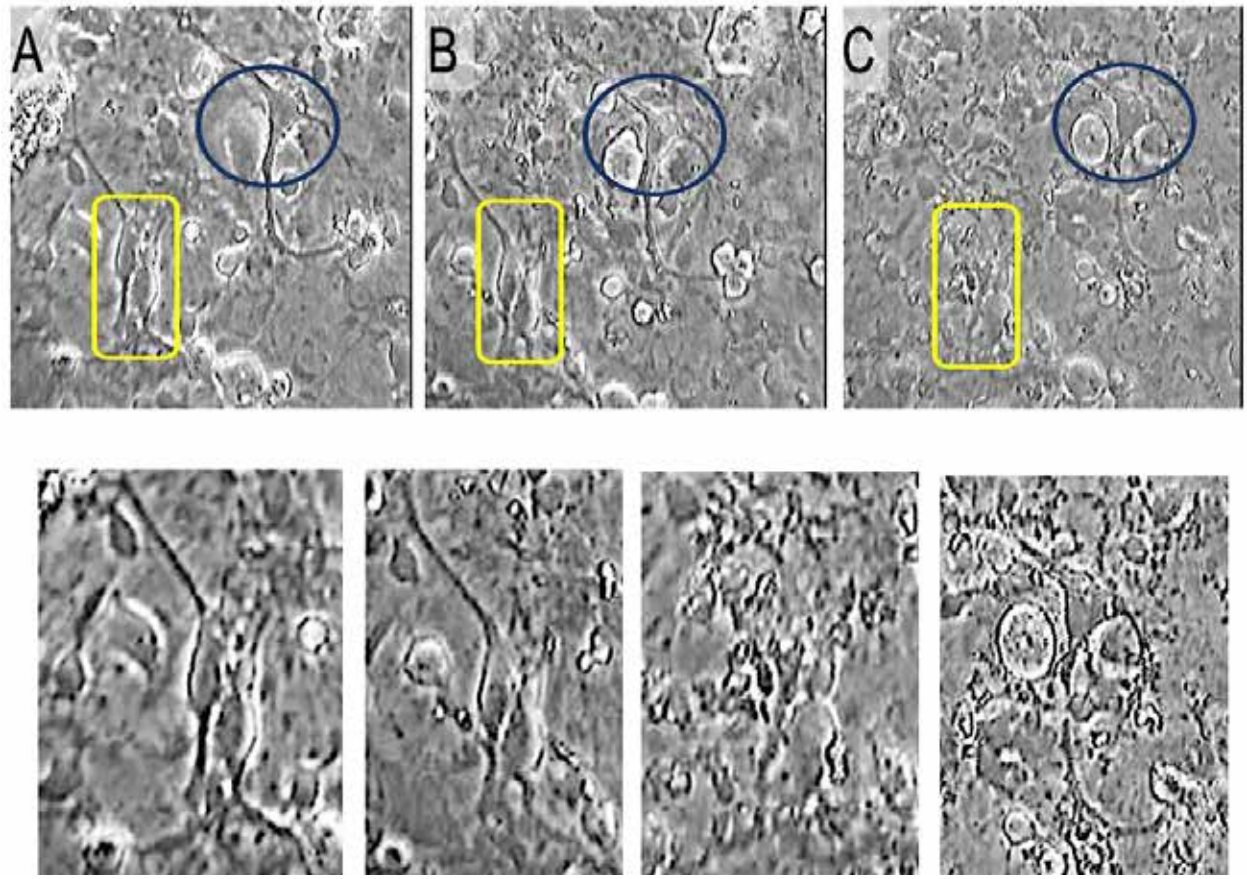

Fig. 3.10. Morphological responses to 50 mM AHQ application on a frontal cortex network. (A) Directly after application (B) One hr after, the yellow box outlines two neurons with loss of processes and cytoplasmic granulation (C) Three hr after, total loss of processes.

In Fig. 3.10, beading of cell body processes is observed in picture B. Total loss of all processes is observed in picture C.

When a 10 mM dose of AHQ was given to the network, an instantaneous response occurred on the morphological level. Lipid protrusions of the membrane began exiting the glial carpet and certain areas of the processes connected to the cell body being followed. Note: at high concentrations, acrolein is a fixative.

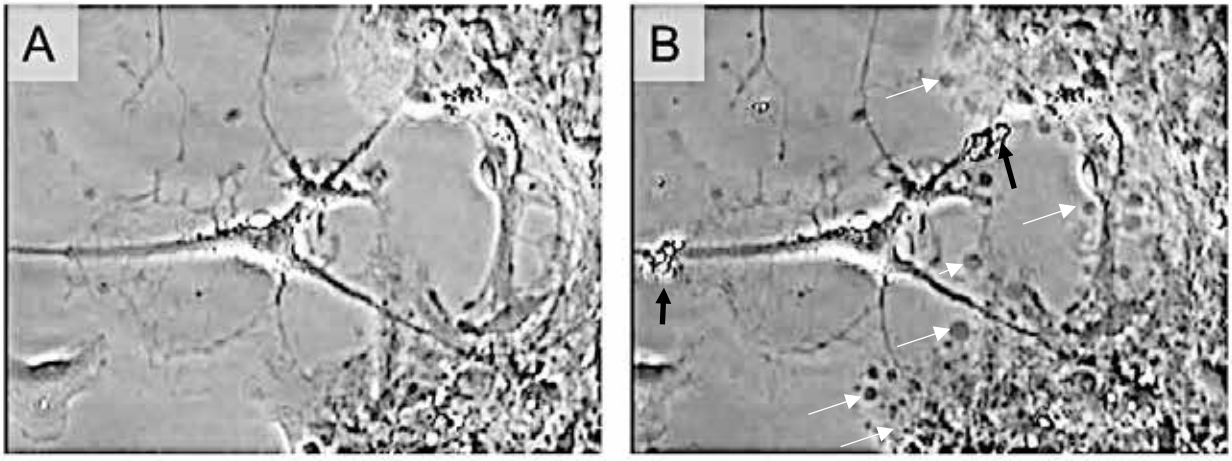

Fig. 3.11. A 10 mM AHQ on a frontal cortex network. (A) Right after 10mM AHQ dose. (B) 5 minutes after dose, lipid bubbles emanate from glia cells (white arrows. Note: Putative disintegration of peripheral dendrites (black arrows).

3.3 Hydroquinone (HQ)

Hydroquinone was a stabilizer in the acrolein used in ADA and AHQ (sections 1 & 2 of results). There is no data for toxicity of this compound on neuronal cultures. To assure that HQ did not interfere with the results in that section. An HQ toxicity screening was conducted for pattern responses in a separate series of experiments. Networks were exposed to 0.1 mM HQ in the 50 mM AHQ experiments.

In the following data, HQ was found to have no effect on network activity in applications lower than 150 mM. However, HQ did show toxicity with a TD_{50} value of 8.6 mM and IC_{50} of 3.5 mM. It also generated instability by inducing intense bursting and showed high and persistent rebound activity after medium changes. For HQ experiments under bicuculline, there were no functional effects until 3.5 mM. The experiments were run with both native networks as well as disinhibited networks with 40 mM bicuculline in serum free medium.

Table 3.3. Table of HQ Experiments

Exp.	Titration mM	Final mM	Channels #	Culture Date	Exp. Date	Age weeks
MA030	5	0.032	10	07.18.17	09.07.17	57
MB030	2.25	0.0175	21	07.18.17	09.07.17	57
MB033	25	0.4	37	10.10.17	11.16.17	35
MA035A	150	1.35	55	10.10.17	11.30.17	49
MB035A	600	1.8	43	10.10.17	11.30.17	49
MA035B	750	7.95	55	10.10.17	11.31.17	50
MB035B	1200	16.08	43	10.10.17	11.31.17	50
MA036	1000	14	18	10.24.17	12.01.17	60

3.3.1 Responses to Low HQ Concentrations

There was no observable effect to 25 mM titrations of HQ up to 400 mM, until receiving a medium change to a medium of identical osmolarlity and pH, without HQ (n=6). The responses were characterized by a massive increase in spike rate that increased the level reference activity with oscillations of super bursting (Suri, master's thesis).

Network pattern changes occurred immediately after medium change. There was an immediate change to coordinated bursting that mimicked the burst pattern of a disinhibited culture.

Applications in ranges ≥ 150 mM HQ exhibit an inhibitory response profile. The inhibition could not be quantified by concentration because applications ranging from 150 mM to 1,800 mM HQ showed the same decrease to minimal activity. However, medium changes induced 400-800% greater activity than reference. The response profile of dramatically increased activity at the time of medium change would last 6-8 hours and be followed by a period of oscillating inhibition (n=3). A second medium

change 12 hours after the first medium change brought reference spike activity back to normal with the same number of active channels (n=1) (Fig. 3.13).

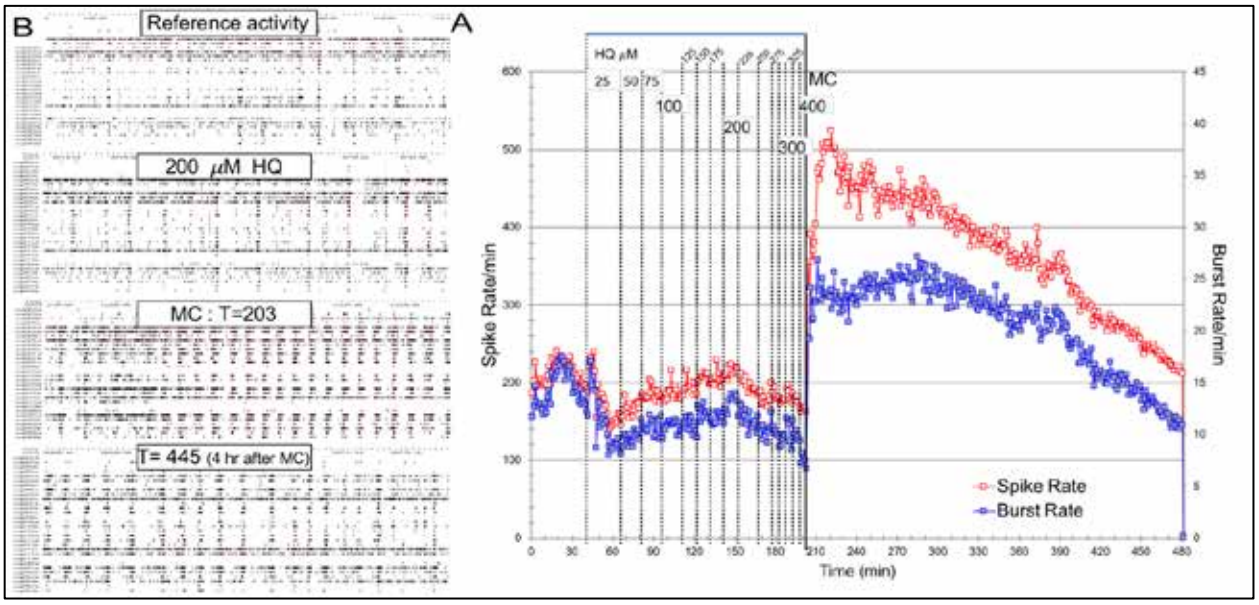

Fig. 3.12. Network changes to multiple additions of HQ. (A) HQ titration from 25 mM – 400 mM. No response in spike rate until a medium change. Rapid increase in spike rate by 400 %(B) Nex roster display of real time spiking shows no pattern changes before (1) and after HQ application (2). Immediately upon removal of HQ by medium change (3), there was a strong change is spike patterns that lasted until a second medium change 12 hours later. (4) 10 min after medium change, (5) 2 hr after medium change. (6) 4 hr. after medium change.

This response profile of increased activity was distinguished by the re-addition of hydroquinone into the network. After being distinguished, it can be induced again by another medium change.

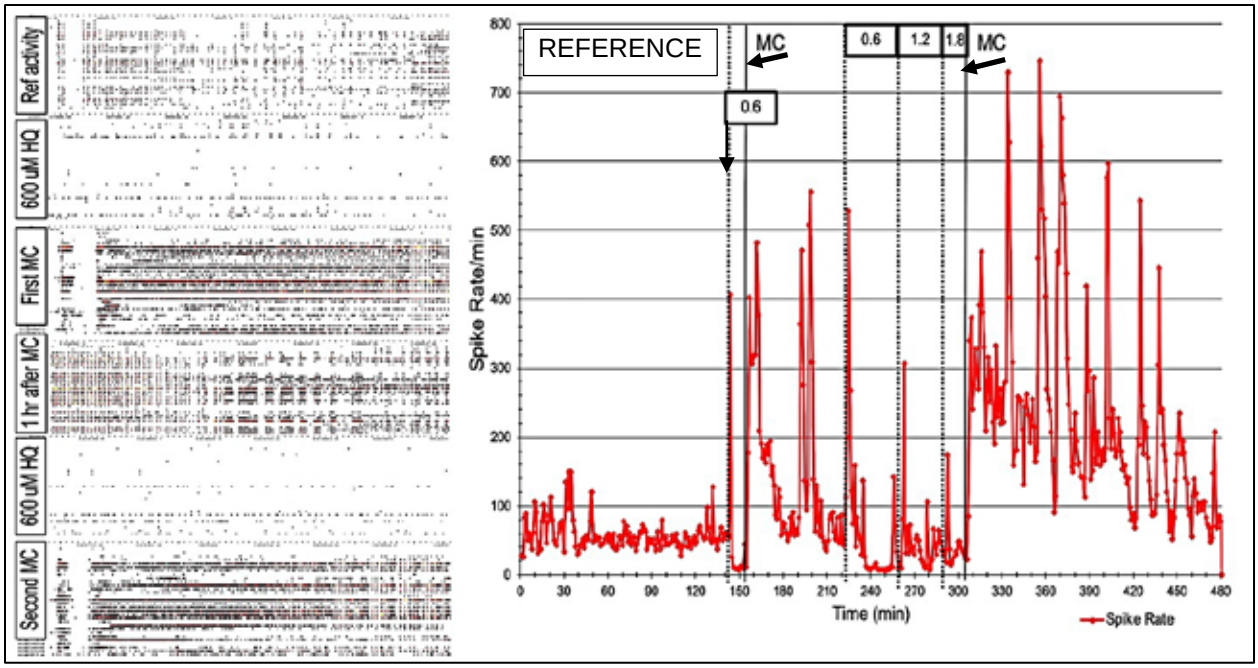

Fig. 3.13. Applications ≥ 150 mM HQ show a decrease in spike rate. This is completely reversible with a medium change and induces a large increase in spike rate and decrease in period between spikes. Network pattern change is reproducible and extinguishable in the same experiment.

3.3.2 Dose Response Curves

Because of the inhibitory response of HQ, 40 mM bicuculline stabilized network activity to quantify its toxicity. Once disinhibited, titrations of HQ showed spike activity decreased at 750 mM with a functional IC_{50} of 1,800 mM and active channels decreased at 5 mM with an LC_{50} of 8.5 mM HQ.

Response profile between a native network and a disinhibited network were dramatically different. Active channels were used to quantify this shift in response to HQ. When plotted with HQ concentration as the dependent variable, the IC_{50} for a native network is 450 mM. The IC_{50} for disinhibited network is 3.5mM.

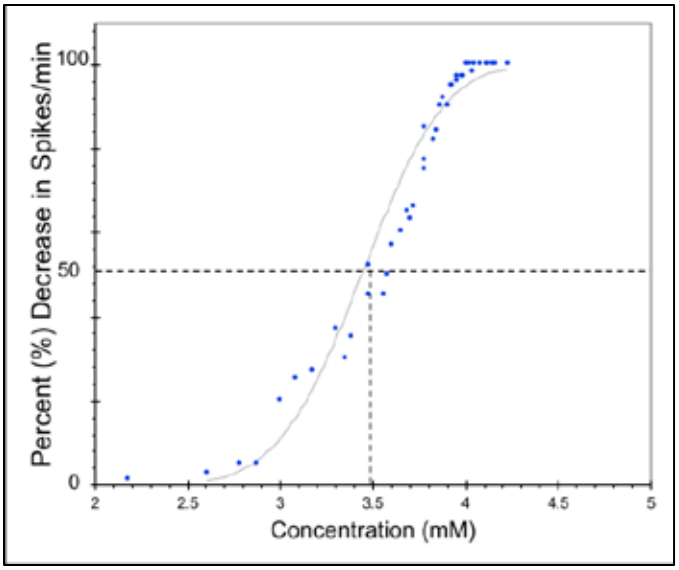

Fig. 3.14. Dose response curve representing all hydroquinone experiments under 40 mM bicuculline (n=6). Dose response curve from all HQ experiment under 40 mM GABA A antagonist. IC_{50} value is 3.5 mM (pooled data from n=5).

3.4 Analytical Acrolein (AA)

Table 3.4. Table of Experiments with Analytical Acrolein

Exp.	Concentration mM	Channels	Culture Date	Exp. Date	Age weeks
MA024	100	40	06.06.17	06.29.17	29
MB024	500	52	06.06.17	06.29.17	29
MB025	85	21	06.06.17	07.04.17	35
MA025	75	50	07.14.17	06.09.17	36
MA028	18.5	27	07.14.17	09.17.17	91
MB028	18.5	22	07.14.17	09.17.17	91
MB029	18.5	55	07.14.17	09.09.17	83
MA031	18	42	10.10.17	11.09.17	29
MB031	18	45	10.10.17	11.09.17	29

3.4.1 Network Response Profiles

Analytical acrolein exhibited a biphasic profile at lethal and nonlethal concentrations. At 30 mM and less, there was no loss in reference activity observed in a 6-day period after application but there was a change in reference spike activity and

patterns that never returned to reference. In one experiment, the change was extinguished with bicuculline 48 hr after 30 mM bicuculline (Fig. 3.18). As concentration increases, time until 100% activity loss decreases.

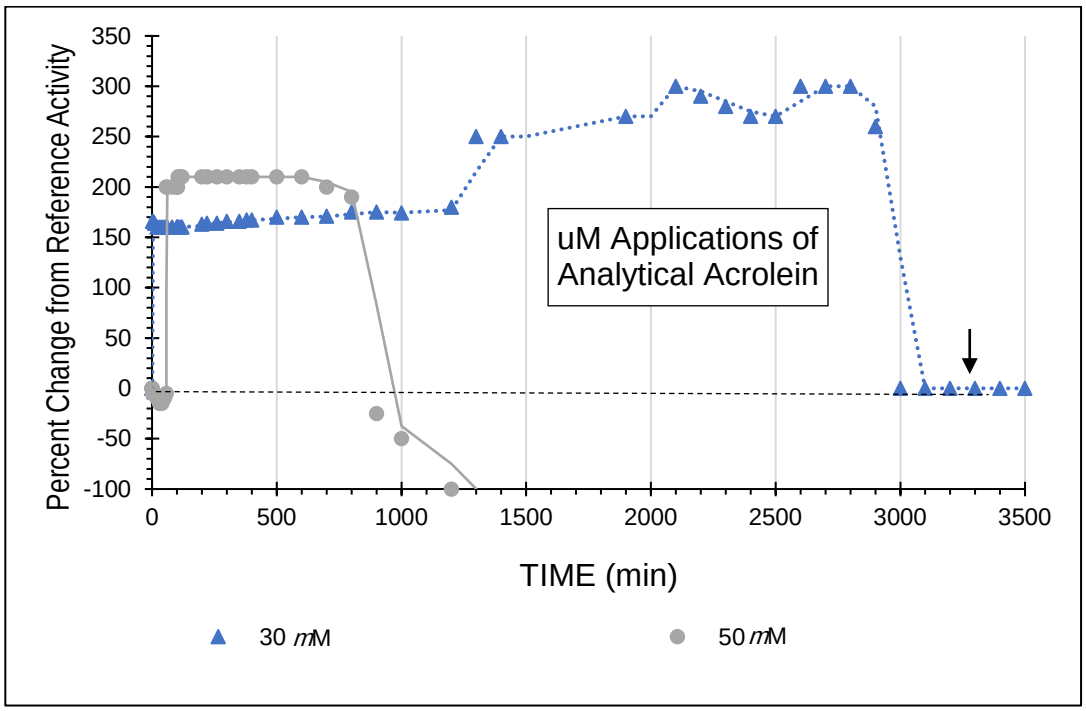

Fig. 3.15. Network activity responses to single analytical acrolein applications in the mM range. Linear plots represent concentration dependent responses. 50 mM, responds with biphasic profile before 100% loss in activity. 30 mM and below (n=3) respond in a biphasic profile with no loss in reference spike activity (arrow).

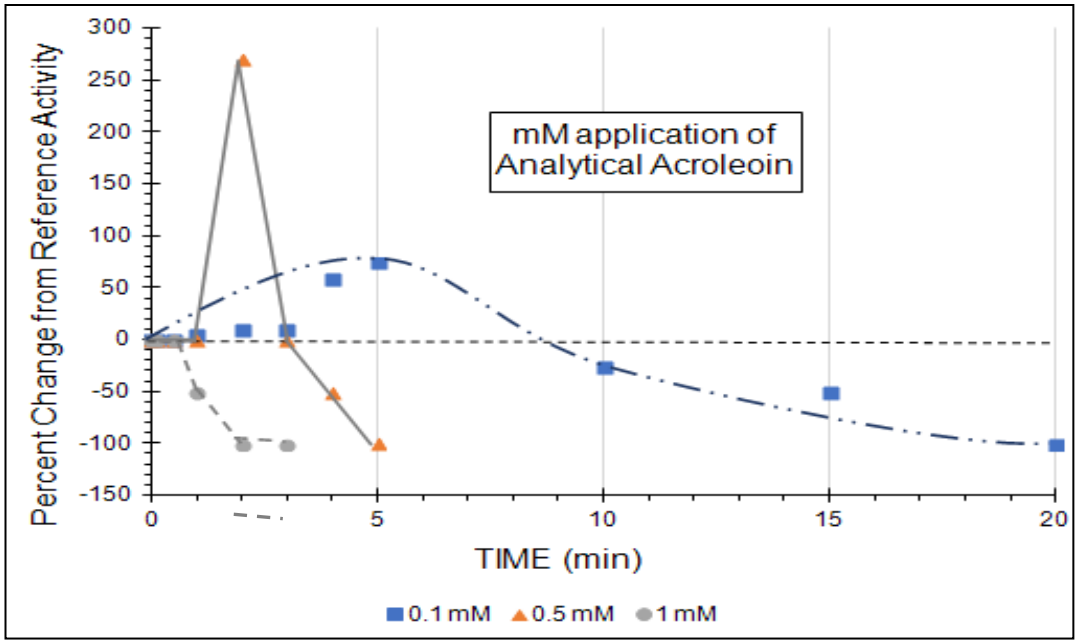

Fig. 3.16. Network activity responses to single analytical acrolein applications in the mM range. In concentration < 1 mM, a biphasic response profile is observed before 100% loss in spike activity.

A linear log-log relationship exists between concentration and time for 100% activity loss. The lower concentrations would be expected to be nonlethal because is a pro-inflammatory compound found inside of mammalian tissue systems in periods of increased stress. The linear range of the sigmoidal plot is confined to 70 mM -1 mM

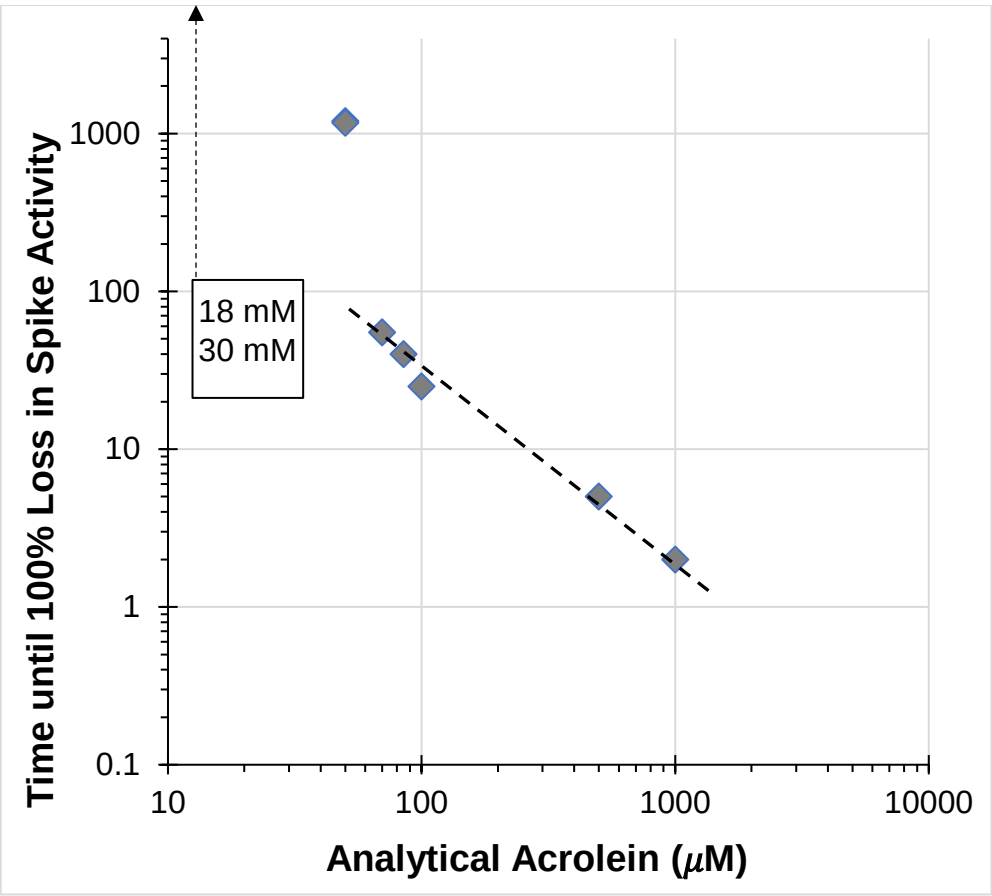

Fig. 3.17. Dose response curve for analytical acrolein. Low concentrations have no effect on loss of activity from reference. As the concentration gets higher the time until 100% loss of activity decreases.

3.4.2 Spike Production and Pattern Changes

Analytical acrolein was the first of the compounds to be examined without bicuculline. The spike production and pattern changes that occurred in these experiments were an increase in burst population rate and coordination. During the second response profile of population burst decrease, coordination is sustained until 100% loss of activity. This is significant of a reduction in ignition site or neural ignition failure.

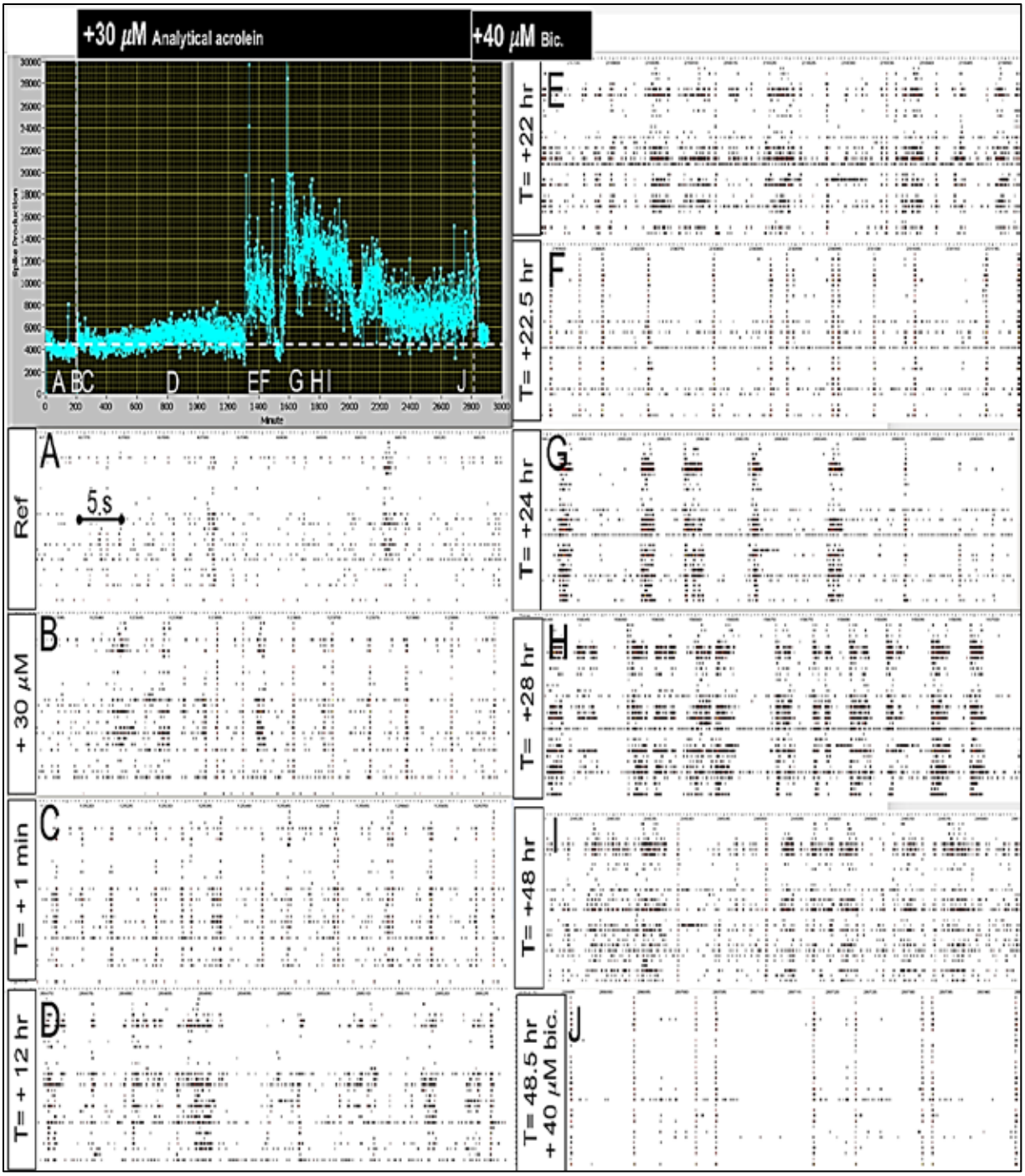

Fig. 3.18. A 30 mM application of analytical acrolein to a network after 2.5 hr of stable reference activity. Network spike production and patterns destabilize and increase for 48 hours until 40 mM bicuculline application at T= + 49 hr. (A) Raster display of reference spike activity of a spontaneously firing network. This was the average activity for the 2.5 hr reference period. (B) Instant change in network spiking after 30 mM application. (C) T= 1 min after, increased burst rate and coordination (D)-(I) continued spike production and pattern change (J) decreased burst rate from 40 mM bicuculline application.

At nonlethal concentrations, pattern changes still occurred that did not return to reference activity in the 6 d observation period (n=2, at 20 mM AA). The pattern change was characterized by an increased population burst rate and coordination. The Spike activity display shows a dramatic increase in the range of total spikes per minute or paroxysmal superbursting. Changes in spike patterns between bicuculline-like bursting and burst packets were observed. The latter increased in width over time. A surprising observation was the pattern stabilization with an addition of bicuculline (see Fig. 3.18).

Higher concentrations, less than 1 mM, had the same response profile of increased burst rate and coordination. This was followed by a death profile of decreased burst rate with sustained coordination until total loss of activity. Fig. 3.19 demonstrates the raster display of this biphasic response.

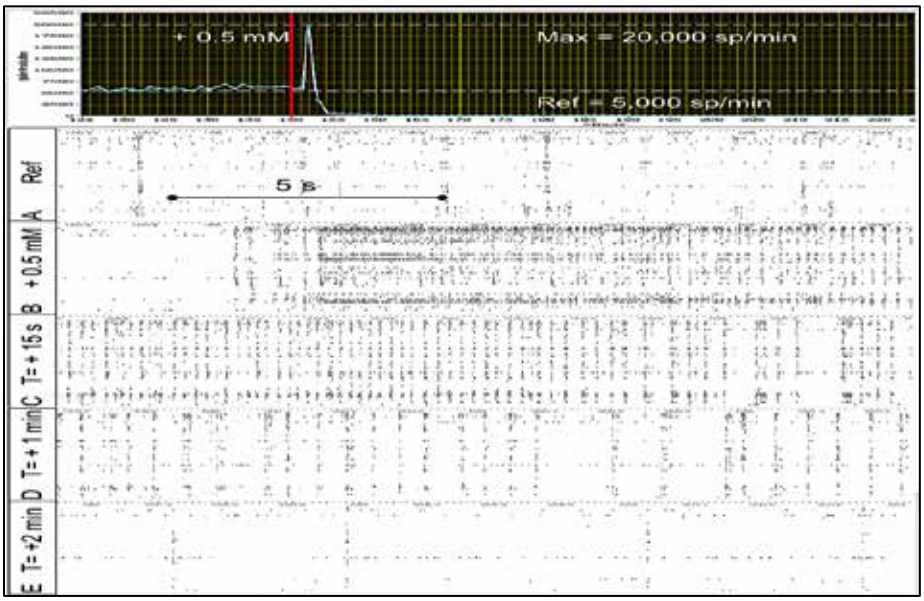

Fig. 3.19. A 0.5 mM analytical acrolein application after 2.5 hr of stable reference activity. (A) native reference activity. (B) application increases burst population rate and coordination. (C-E) the rate of population bursts decreases from 108 bpm to 16 bpm. This implies loss of ignition site or greatly reduced ignition site activity.

Once analytical acrolein is applied into the network, spontaneous reference spike activity immediately increases, and gains coordination shortly thereafter. This coordination is maintained when the burst rate begins to decrease. This same profile is seen concentrations ranging from 50 mM -0.5 mM. The observed death profile is that of either reduction in ignition sites or neural ignition failure (Ham et al., 2008). Very few channels fire outside of the bursts which have full participation.

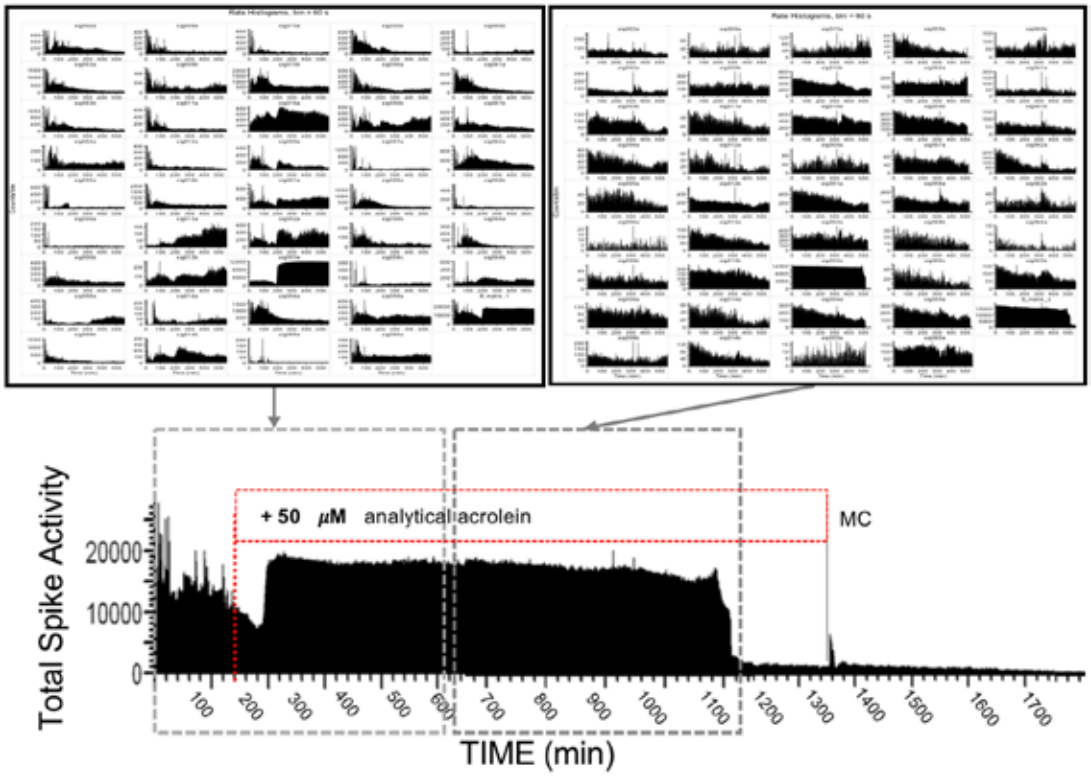

Fig. 3.20. A 50 mM application of analytical acrolein to a spontaneously firing network. (Top) Individual channel spike activity for 3 segments of Plexon data. The Y axis is total spikes per minute generated by a channel and the x axis is time in minutes. (Bottom) Total spike activity for the entire network. After a 50 mM application, some channels have an inhibitory profile while other an excitatory until total loss in activity.

3.4.3 Waveshape Analysis

Wave shapes were recorded by Plexon with timestamps (μSec) that can be

extracted in order to display wave shapes for certain reference periods within the experiment. Because the wave shapes would visible grow on the Plexon channel display window after acrolein application, the waveshapes were analyzed further.

In analyzed wave shapes, a 25-35% increase in amplitude is observed (Fig. 3.21). In applications of small concentrations, experiment protocols report new wave shapes appearing in the channel selection after application. The narrowing of the peaks paired with increased amplitude are common observations when there is a shift in Na^+ permeability.

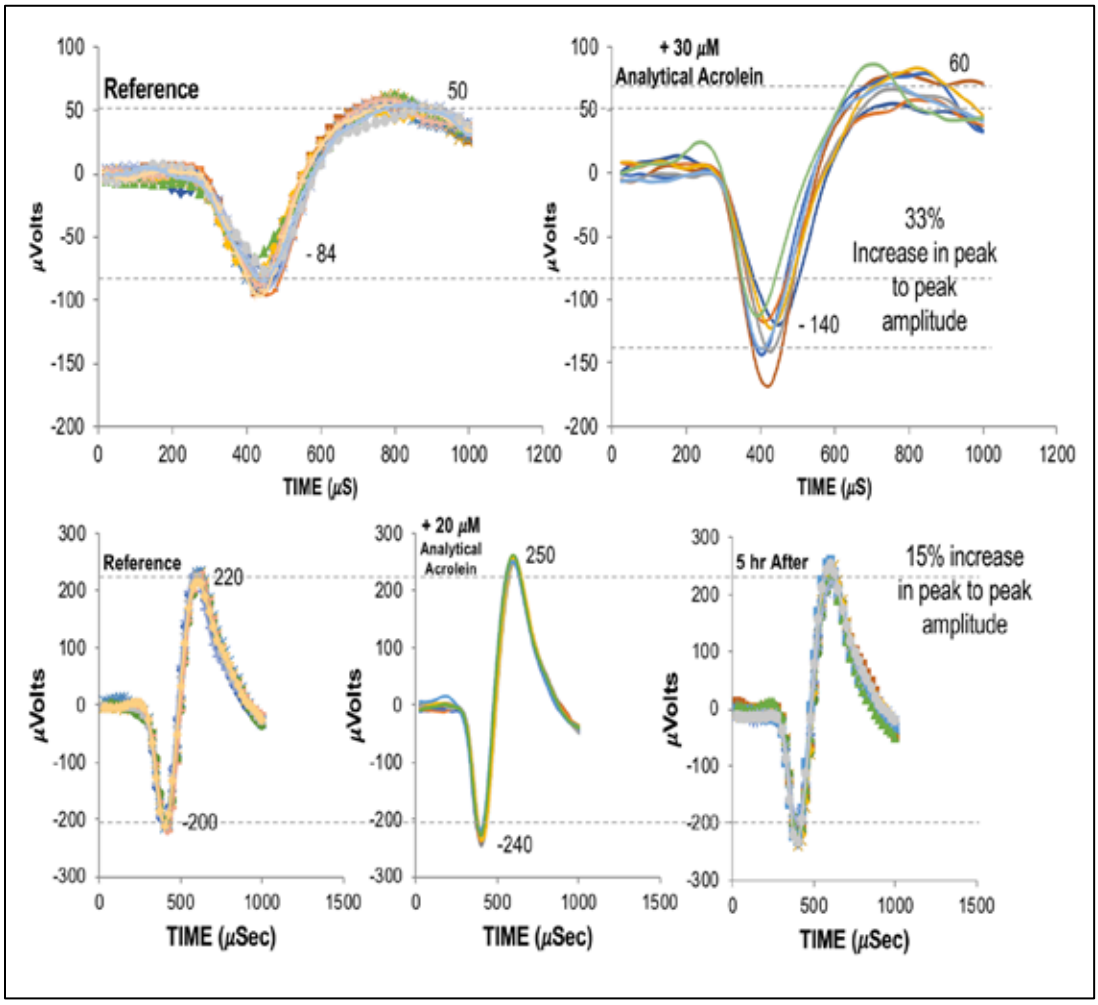

Fig. 3.21. A 20 and 30 mM analytical acrolein application increases the action potential amplitude in minutes and continues to slowly increase over the first phase profile of analytical acrolein.

3.5 Summation of Acrolein Data

The summation of acrolein data on a single graph shows a relationship between each compound and the time until 100% activity loss is plotted in Fig. 3.22. At 400 mM, the respective IT_{100} values are 6 minutes for analytical acrolein, 12 minutes for AHQ, and 28 minutes for ADA. The decreased IT_{100} value would be expected for analytical acrolein, which has no stabilizer present.

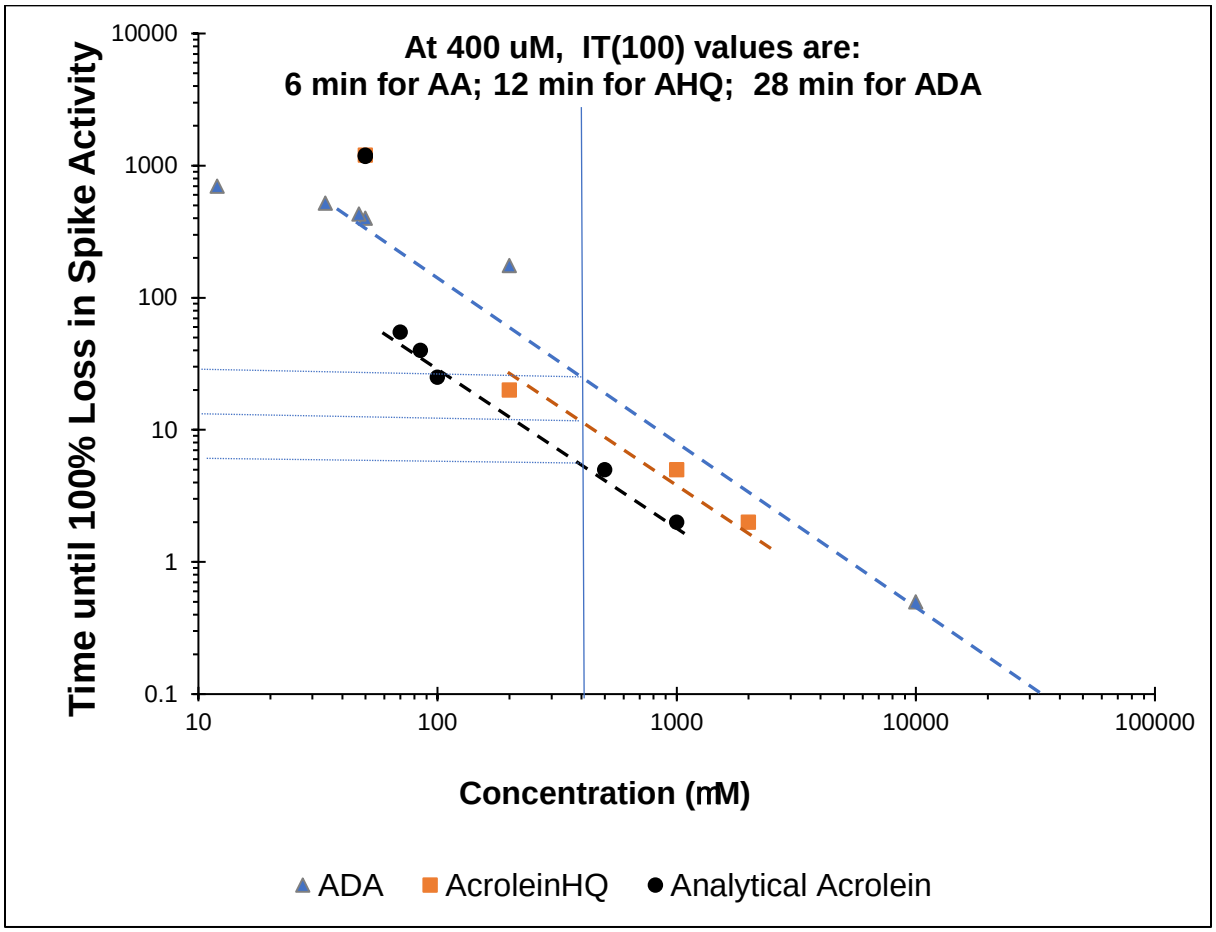

Fig. 3.22. All acrolein compounds used in results section prior are summated. Only lethal concentrations are used in this data set. ADA and AHQ have 40 mM bicuculline, analytical acrolein does not). Linear trend lines are self-drawn.

CHAPTER 4

DISCUSSION

4.1 Acrolein

Analytical acrolein experiments did not achieve the desired iterations due to a supplier shortage. The applications with analytical acrolein did not have bicuculline for stabilization but retained the same observed responses as ADA and AHQ (which contained 40 mM bicuculline). Analytical acrolein had the lowest IT_{100} values, which would be expected of an autooxidant that is not stabilized.

For all three compounds: a biphasic response is observed beginning with a period of increased population burst rate. In experiments with 40 mM bicuculline, coordination was present in the reference and maintained. In the analytical acrolein applications (without bicuculline), coordination would appear after a 5.0-10.0 sec period of abnormally high, full network spiking. The increase in population burst rate was observed in each acrolein compound that was tested, except at very high concentrations when rapid activity loss dominated the initial increase of activity and those with 5% serum.

The second phase is characterized by a decrease in population burst rate with sustained coordination until 100% activity loss for all three compounds. Burst durations and spikes in bursts also decreased, contributing to the loss of activity with time.

The paradoxical effect of acrolein, an increased potency in the presence of serum, was observed in ADA and AHQ (see Figs 4 & 10). Acrolein has been shown to react with many systemic proteins via the Mailard reaction. These reaction products cause apoptosis and necrosis in cell culture (Conklin et al., 2012). Reaction products

have not yet been studied in functional networks but may be toxic by interacting with membrane receptors and channels that control spike production.

One mechanism for the initial increase in activity in acrolein experiments is spermine, a free radical scavenger. Free concentrations of spermine decrease once acrolein has been generated endogenously because of adduction to free radicals and acrolein (Ha et al., 1998; Tsuisui et al., 2016). In normal mM concentrations, spermine has little effect on NMDA receptor/channel complex or voltage gates Na^+ channels. Upon shifting to low levels in the range of 1.0-10 mM, there is an increase in NMDA channel opening frequency in primary cortical cultures (Rock & Macdonald, 1992).

Other important cellular defenses against electrophilic compounds, such as glutathione transferase, become depleted rapidly after the generation of acrolein (Shi et al., 2011). In patients with kidney disease, there is a depletion in spermine levels from serum. Putrescine, polyamine oxidase and acrolein are increased during this period (Igarashi et al, 2006). Acrolein is continuously generated by spermine oxidase, which serves to deplete spermine levels (Igarashi et al., 2011).

Waveshape data shows an increase in peak to peak amplitude in the three experiments that have been examined (Fig. 3.21). Shifts in Na+ permeability increases the action potential peak to peak amplitude. Spermine depletion to low concentrations influences Na^+ channels leading to an increase in spontaneous spiking and hyper-synchronized discharge in cortical neurons (Fleidervish et al., 2008). This is a mechanism that should be researched further, as AP amplitude increases can enhance exocytosis and network excitation.

Fig. 4.1 depicts a 30 mM application of analytical acrolein that induced an increase in population burst rate with coordination over 48 hours. This increased burst rate was extinguished by the addition of 40 uM bicuculline. There is no explanation for this response to a $GABA_A$ antagonist.

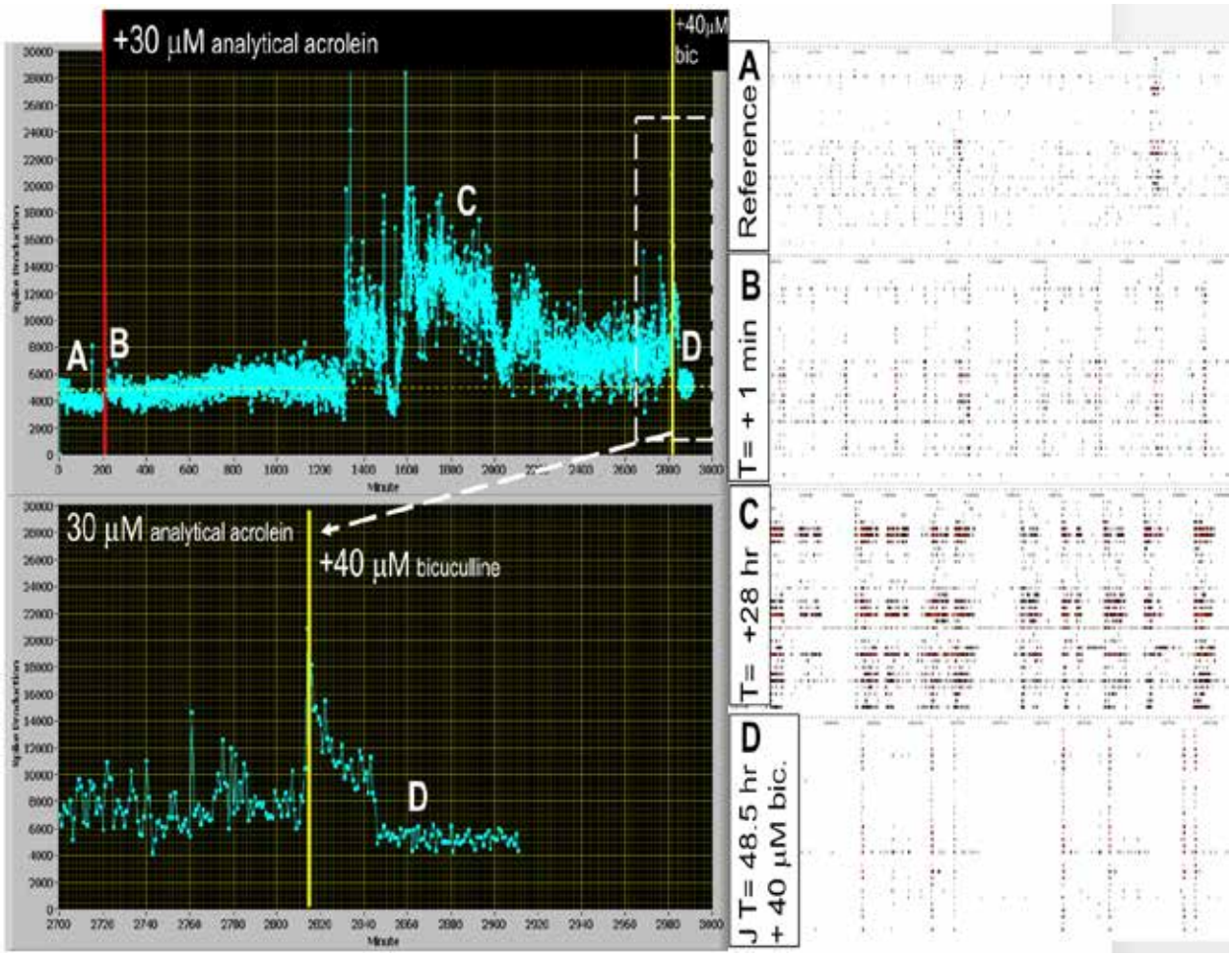

Fig. 4.1. A network response to a 30 mM application of analytical acrolein. The upper Vernac display is the entire 50 hr. recording. A-D: network activity with correlated 15 sec spike raster plots. The bottom panel shows the activity transition from a 40 mM bicuculline application (48 hours after acrolein). (A) Reference network activity. (B) One minute after application. (C) Twenty-eight hr. after application, sudden transition to paroxysmal bursting with appearance of burst packets. (D) A 40 mM bicuculline application decreases population burst rate while maintaining coordination. Total network spike production shows high stability.

4.2 Hydroquinone

Because HQ is a stabilizer for ADA and AHQ, a toxicity screening was necessary to determine independent pharmacological influences of HQ. The final concentration of HQ in the medium bath of ADA and AHQ experiments is listed in Table 4.1. These bath concentrations are far below the concentrations that have shown independent activity changes (Fig. 3.12). In the presence of 40 mM bicuculline, HQ generates no measurable spike rate changes until 2.5 mM (2,500 mM).

Table 4.1. Final HQ Concentration in Acrolein Experiments

10 mM ADA	0.00608 mM HQ
1,000 mM ADA	0.06080 mM HQ
1,000,000 mM ADA	60.800 mM HQ
10 mM AHQ	0.01904 mM HQ
1,000 mM AHQ	1.90400 mM HQ
2,000 mM AHQ	3.80800 mM HQ

At concentrations of 30 mM - 2,000 mM HQ, a medium change induces a 400-800% increase in activity with superbursting. This network pattern change has been seen as late as 6 hours after medium change.

4.3 Conclusion

If post TBI-induced excitotoxicity was only a manifestation of excess glutamate in the synapse, then NMDA, ampa, and kainite receptor antagonists should show success in treatment of secondary damage (Ikonomidou, 2002; Shohami et al., 2014). The literature has shown that it does not.

Cebak et al., 2016 found that phenylalazine, a free radical scavenger, not only successfully mitigated acrolein formation, but attenuated mitochondrial respiratory

dysfunction in a mouse TBI model. Along with the continued study of functional changes that arise from acrolein in a spontaneously firing network, the functional toxicity for hydralazine and phenylalazine applications should be reviewed as well.

Changes in polyamine levels after traumatic brain injury should also be investigated further. Polyamines are essential for eukaryotic growth and development. Deregulation in polyamines is associated with many diseased states (Minois et al, 2011). Polyamines are also important in regulation of glutamate receptor ion channels, inwardly rectifying K^+ channels, and other channels that affect intracellular calcium signaling or Na^+ transport (Dingledine et al., 1999; Stanfield & Sutcliffe, 2003). If there is a change in the polyamines after TBI and acrolein generation, this is another avenue of exploration for pharmaceutical intervention.

This study characterized how acrolein induces but also terminates spike production when applied to spontaneously firing cortical networks. There is no current literature about the functional toxicity of cortical neuronal networks to acrolein, even though it has been shown to enhance and prolong secondary damage in TBI (Cebak et al., 2016). Acrolein and its functional responses should be researched further for efficient intervention and better long-term outcomes of TBI patients.

APPENDIX A

DEFINITIONS AND ACRONYMS

AHQ—Acrolein stabilized in 10% hydroquinone

AO – Amine oxidase: and enzyme responsible for catalyzing the formation of polyamines

ADA—Acrolein diethyl acetate

Bicuculline—$GABA_A$ antagonist. Disinhibits network at 40 mM.

Active channels—Channels with ten or more spikes per minute

CNNS – Center for Network Neuroscience

D1SGH – Dextrose-1 Sucrose Glucose Hepes: buffer solution with balanced ions for biological tissue

DIV – Days in vitro

DMEM – Dulbecco's modified medium: nutritional solution for cell culture
HQ—Hydroquinone, a reducing agent

IC_{50} – Concentration that causes 50% inhibition in spikes/min

IC_{100} -- Concentration that causes 100% inhibition in spikes/min

IT_{100} – Time until 100% inhibition after the application of a compound at X concentration

NMDA receptor – N-methyl-D-arspartate receptor: an excitatory receptor, commonly activated by glutamate

MC—Medium change. Medium is carefully aspirated via a syringe and then replaced by a new medium of the same osmolarity and pH.

MEA – Micro electrode array: the recording area consisting of many substrate-integrated microelectrodes for simultaneous, extracellular recording from many sites in a network.

Mean spikes per min: the average amount of spikes produced each minute by each individual unit

ROS – Reactive oxygen species: A chemical species which is highly reactive and contains an oxygen atom

T – Time: time in minutes

TC_{50} – Toxic concentration for 50% of the channels

TBI – Traumatic brain injury: an insult to the brain caused by external physical force

Titration – a single application given in a series of applications to elucidate a dose response

Total spikes per min: Total spikes produced each minute by individual units

Serum—Donor horse serum that is heat deactivated by proprietary source as well as within the lab.

SO – Spermine oxidase: an enzyme responsible for catalyzing the formation of spermine.

Spk – Spike: A single action potential

APPENDIX B

SOLUTION SOURCE CONCENTRATION CALCULATIONS

Acrolein Diethyl acetate (stabilized in 4% hydroquinone) (ADA) Solutions

Source solution: 0.854 g / ml, 25.0 ml volume

0.854 x 1000 ml = 854 g / L

854 g / MW 130.18 = 6.57 M ADA Source

Acrolein (stabilized in 10% hydroquinone) (AHQ) Solutions

Source solution: 0.839 g / ml, 25.0 ml volume

0.839 x 1000 ml = 839 g / L

839 / MW 56.06 = 14.97 M AHQ Source

Analytical Acrolein Solutions

Source solution: 0.839 g / ml, 25.0 ml volume

0.839 x 1000 ml = 839 g / L

839 / MW 56.06 = 14.97 M analytical acrolein Source

REFERENCES

Biegon, A., Fry, P. A., Paden, C. M., Alexandrovich, A., Tsenter, J., & Shohami, E. (2004). Dynamic changes in n-methyl-d-aspartate receptors after close head injury in mice: implications for treatment of neurological and cognitive deficits. *PNAS*. 101(14), 5117-5122

Beigon A., Fry P. A., Alexandrovich A., Isenter J., & Shohami E. (2004). *Bn. Proc. Natl. Acad. U.S.A*. 101,5117-5122

Bromfield, E. B., Cavazos, J. E., Sirven, J. I. (2006). An Introduction to Epilepsy [Internet]. West Hartford (CT): *American Epilepsy Society. Chapter 1, Basic Mechanisms Underlying Seizures and Epilepsy.* Retrieved from: https://www.ncbi.nlm.nih.gov/books/NBK2510/

Bullock, R., Kuroda, T., Teasdale, G. M., & Muculloch, J. (1992). Prevention of post-traumatic excitotoxic brain damage with NMDA antagonist: a new strategy for the nineties. *Acta Neurochir*. 55, 49-55

Bullock, R., Zauner, A., Woodward, J. J., et al., (1988). Factors affecting excitatory amino acid release following severe human head injury. *J Neurosurg*. 89, 507-518

Caldwell, R. B., Toque, H. A., Narayanan P. S., Caldwell, R. W. (2015). Arginase: and old enzyme with new tricks. *Trends in Pharmacological Sciences*. 26(6), 395-405

Cebak, J. E., Sinh, I. N., Hill, R. L, Wang, J. A., & Hall, E. D. (2016). Phenelzine protects brain mitochondrial function *in vitro* and *in vivo* following traumatic brain injury by scavenging the reactive carbonyls 4-hydroxynonenal and acrolein leading to cortical histologica neuroprotection. *Journal of Neurtrauma*. Online ahead of print.

Cerevelli, M., Bellini, A., Bianchi, M., Marcocci, S., Nocera, F., Polticelli, R., Federico, R., Amendola, & R., Mariottini, P. (2004). Mouse spermine oxidase gene splice variants. Nuclear subcellular localization of novel active isoform. *European Journal of Biology*. 271,760-770

Conklin, D. J., Barski, O. A., Lesgards, J. (2010). Acrolein consumption induces systemic dyslipidemia and lipoprotein modification. Toxicol Appl Pharmacol. 243,1–12.

Dingledine, R., Borges, K., Bowie, D. & Traynelis, S. F. (1999). The glutamate receptor ion channels. *Pharmacol Rev.* 51(1),7-61.

Fleidervish, I. A., Libma,n L., Katz, E., & Gutnick, M. J. (2008). Endogenous polyamines regulates cortical neuronal excitability by blocking voltage gated Na+ channels. *PNAS*. 105(48): 18994-18999

Guerriero, R. M., Giza, C. C., & Rotenberg, A. Glutamate and GABA imbalance following traumatic brain injury. *PMC*. 15(5), 27

Ghilarducci, D. P. & Tjeerdema, R. S. (1995). Fate and effects of acrolein. *Rev Environ Contam Toxicol*. 144,95–146.

Greve, M. & Zink, B. J. (2009). Pathophysiology of traumatic brain injury. 76(2), 97-104

Gross, G.W. (1979). Simultaneous single unit recording in vitro with a photoetched laser deinsulated gold multi-microelectrode surface*. IEEE Trans. Biomed. Eng.* 26, 273–279.

Gross, G.W., Wen, W. & Lin, J.1(985). Transparent indium-tin oxide patterns for extracellular, multisite recording in neuronal cultures. *J. Neurosci. Meth* 15, 243–252.

Gross, G.W. & Schwalm, F.U. (1994). A closed chamber for long-term electrophysiological and microscopic monitoring of monolayer neuronal networks*. J. Neurosci. Methods.* 52, 73–85.

Gross, G.W., Azzazy, J.M.E., Wu, M.C. & Rhoades, B.K. (1995). The use of neuronal networks on multielectrode arrays as biosensors. *Biosens. Bioelectron.* 10, 553–567.

Gross, G. W., Rhoades, B. K., Reust, D. L., & Schwalm, F. U. (1993). Stimulation of monolayer networks in culture through thin film indium-tin oxide recording electrodes. *Journal of Neuroscience Methods. 50*, 131-143.

Gross, G.W & Gopal., K.V. (2006) Emerging histiotypic properties of cultured neuronal networks. In: M. Taketani and M. Baudry (eds) Advances in Network Electrophysiology using Multi-Electrode Arrays. Springer, 193-214.

Ha H. C., Sirisoma N. S., Kuppusamy P., Zweier J. L., Woster P. C. & Casero R. Jr. (1998). The polyamine spermine functions directly as a free radical scavenger. *Biochemistry. Proct. Nat. Acad. Sci*. 95,11140-11145

Ham, M., Bettencourt, L., McDaniel, F. D. & Gross, G. W. (2008). Spontaneous coordinated activity in cultured networks: analysis of multiple ignition sites, primary circuits, and burst phase delay distribution. Journal of Computational Neuroscience. 24,346-357

Hynd, M. R., Scott, H. L. & Dodd, P. R. (2004). Glutamate-mediated excitotoxicity and neurodegeneration in Alzheimer's disease. *Neurochemistry international.,* 45(5), 583-595l

Igarashi, K., Ueda, S., Yoshida, K. & Kashiwagi, K. (2006). Polyamines in renal failure. Amino Acids.31,477–483

Igarashi ,K. & Kashiwagi, K. (2011)Protein-conjugated acrolein as a biochemical marker of brain infarction. *Mol. Nutr. Food Res.* 55,1332–1341

Ikonomidou, C. & Turski, L. (2002). Why did nmda antagonists fail clinical trails for stroke and traumatic brain injury?. *Lancet Neurol*. 1(16),383-386.

Johnstone, A. F.M., Gross G. W., Weiss, D. G., Schroeder, O., Gramowski, A. & Shafer, T.J. (2010)

Micro-electrode Arrays: A Physiologically-based Neurotoxicity Testing Platform for the 21st Century. *NeuroToxicology*. 31, 331–350.

Krishnamurthy, K. & Laskowitz, D. T. (2016).Chapter 5 cellular and molecular mechanisms of secondary neuronal injury following traumatic brain injury. *Translational Research in Traumatic Brain Injury.* Boca Raton (Fl). CRC Press/Taylor and Francis Group.

Landgehem, F. K. H., Weis, T., Oehmichen, M. & Diemling, A. (2006). Decreased expression of glutamate transporters in astrocytes after human traumatic brain injury. *Journal of Neurotrauma*. 23(10), 1518-1528

Langer, M., Brandt, C., Zellinger, C. & Loscher W. (2011). Therapeutic window for the neuroprotective efect of valproate versus the competitive AMPA receptor antagonist NS1209 following status epilepticus in rats. *Neuropharmacology*. 61(5-6),1033-1047

Lai, T. W., Zhang, S. & Wanh, Y. T,. 2013. Excitotoxicity and stroke: identifying novel targets for neuroprotection. *Progress in Neurobiology*. 115, 157-188

LoPachin, R. M. & Gavin, T. (2014). Molcular mechanisms of aldehyde toxicity: A chemical perspective. *Chem Res Toxic.* 27(7),1081-1091

Liddelow, S. A., Guttenplan, K. A., Clarke, L. E., Bennet, F. C., Bohlen, C. J., Schirmer, L., Bennet, M. L., Munch, A. E., et al., (2017). Neurotoxic reactive astrocytes are induced by activated microglia. *Nature.* 541, 481-487

Lin, C-L. G., Kong, Q., Cuny, G. D., Glicksman, M. A. (2013). Glutamate transporter EAAT2: a new target for the treatment of neurodegenerative diseases*. Future Med Chem*. 4(13), 1689-1700

LoPachin, R. M. & Gavin, T. (2014). Molecular mechanisms of aldehyde toxicity: a chemical perspective. *Chem res Toxicol.* 27(7),1081-1091

Minois, N,, Carmona-Gutierrez, D. & Madeo, F. *(2011).* Polyamines in aging and disease. *Aging (Albany NY). 3(8),716-32*

Morris B. & Mayer M. L. (1993). Multiple effects of spermine on N-methyl-D-aspartatic acid receptor respones of rat cultured hippocampal neurons. *Laboratory of Cellular and Molecular Physiology.* Bethesda, MD. 464, 131-163

Patel, C., Xu, X., Shosha E., Xing, J., Lucas, R., Caldwell, R. W., Cadwell, R. B. & Narayanan, S. P. (2016). Treatment with polyamine oxidase inhibitor reduces microglial activation and limits vascular injury in ischemic retinopathy. *Biochimica et Biophysica Acta (BBA Molecular Basis of Disease*. 1862(9), 1628-1639

Penney, K. B., Smith C. J. & Allen, J. C. (1984). Depigmenting Action of Hydroquinone Depends on Disruption of Fundamental Cell Processes. *Journal of Investigative Dermatology. 82(4),308-310*

Potter, S. M. & DeMarse, T. B. (2001). A new approach to neural cell culture for long-term studies. *Journal of Neuroscience Methods, 110,* 17-24.

Rothman, S.M. (1983). Synaptic activity mediates death of hypoxic neurons. *Science*. 220, 536–537

Rock, D. M. & Macdonald R. L. (1992). The polyamine spermine has multiple actions on N-methyl-D-aspartate receptor single-channel currents in cultured cortical neurons. *Molecular Pharmacology. 41 (1,) 83-88*

Sharmin, K., Sakata, K., Kashiwaga, S., Ueda, S., Iwasak, A. & Shirahata ,A. (2001). Polyamine cytotoxicity in the presence of bovine serum amine oxidase. *Biochem. Boiphys. Re. Comm.* 282, 228-235

Shi, R., Page, J. & Tully, M. (2015). Molecular mechanisms fo acrolein-mediated myelin destruction in CNS trauma and disease. 49(7), 888-895

Shi, R., Rickett, T., & Sun, W. (2011). Acrolein-mediated injury in nervous system trauma and diseases. *Molecular Nutrition & Food Research*. *55*(9), 1320–1331

Shohami, E. & Beigon, A. (2014). Novel approach to the role of NMDA receptors in traumatic brain injury. *CNS NEurol Disord Drug Targets*. 13(4), 567-573

Sloviter, R. S. 2011. Progress on the issue of excitotoxic injury modification vs. real neuroprotection; implications for post traumatic epilepsy. *Neuropharmacology*. 61(5-6),1048-1050

Stanfield, P. R. & Sutcliffe, M. J. (2003). Spermine is fit to block inward rectifier (Kir) channels. *J Gen Physiol.* 122(5),481-4

Stevens J. F. & Maier C. S. (2008). Acrolein: sources, metabolism and biomolecular interactions to human health and disease. *Mol Nutr Food Res.* 52(1), 7-25

Sullivan, P. G., Keller, J. N., Mattson, M. P. & Scheff S. W. (1998). Traumatic brain injury alters synaptic homeostasis: implications for impaired mitochondrial and transport function. *Journal of Neurotrauma*. 15,789-798

Tomotori, H., Usui, T., Saeki, N., Ueda, S., Kase, H., Nishimura, K. & Kashiwagi, K. (2005). Polyamine oxidase and acrolein as novel biochemical markers for diagnosis of cerebral stroke. *Stroke*. 36, 2609-2613

Tsutsui, A., Imamaki, R., Kitazume, S., Hanashima, S., Yamaguchi, Y., Kaneda, M., Oishi, A., Fuhii, N., Kurbangalieva, A., Taniguchi, N. & Tanaka, K. (2014). Polyamine modification by Acrolein exclusively produces 1,5-diazacyclooctanes: a previously unrecognized mechanism for Acrolein mediated oxidative stress. *Organic and Biolmolecular Chemistry*. 12, 5151

Wang, C., Delcros, J. & Cannon, L. (2003). Defining the molecular requirements for the selective delivery of polyamine conjugate in cells containing active polyamine transporters. *Journal of Medical Chemistry*. 46(24), 5129-5138

Werner C., Engelhard K. (2007). Pathophysiology of traumatic brain injury. *Brit J Anaesth*. 99(1),4-9

Wood, P., Knan, M., Moskal, J. (2007). The concept of “aldehyde load” in neurodegenerative mechanisms: cytotoxicity of the polyamine degradation products hydrogen peroxide, Acrolein, 3-aminopropanal, 3acetamidopropanal and 4-aminobutanal in a retinal ganglion cell line*. Brain Research*. 1145, 150-156

Yi J. & Hazell A. S. (2006). Excitotoxic mechanism and the role of astrocytic glutamate transporters in traumatic *brain injury*. 48(5),394-403

Zappia, V., Cacciapuoti, C., Pontoni, G. & Olvia, A. (1980). Mechanisms of propylamine-transfer reactions. *Journal of Biological Chemistry*. 255(15), 7276-7280